LAWRENCE
LIVERMORE
NATIONAL
LABORATORY

LLNL-JRNL-407811

Evidence for Cardiomyocyte Renewal in Humans

O. Bergmann, R. D. Bhardwaj, S. Bernard, S. Zdunek, F. Barnabe-Heider, S. Walsh, J. Zupicich, K. Alkass, B. A. Buchholz, H. Druid, S. Jovinge, J. Frisen

October 15, 2008

Science

Disclaimer

Evidence for cardiomyocyte renewal in humans

Olaf Bergmann[1,*], Ratan D. Bhardwaj[1,*], Samuel Bernard[2], Sofia Zdunek[1], Fanie Barnabé-Heider[1], Stuart Walsh[3], Joel Zupicich[1], Kanar Alkass[4], Bruce A. Buchholz[5], Henrik Druid[4], Stefan Jovinge[3, 6] and Jonas Frisén[1]

[1]Department of Cell and Molecular Biology, Medical Nobel Institute, Karolinska Institute, SE-171 77 Stockholm, Sweden. [2]CNRS UMR5208, Institut Camille Jordan, Université Claude Bernard Lyon 1, France. [3]Lund Strategic Research Center for Stem Cell Biology and Cell Therapy, Lund University, SE-221 84 Lund, Sweden. [4]Department of Forensic Medicine, Karolinska Institute, SE-171 77 Stockholm, Sweden. [5]Center for Accelerator Mass Spectrometry, Lawrence Livermore National Laboratory, 7000 East Ave., L-397, Livermore, CA 94551 USA. [6]Department of Cardiology, Lund University Hospital, SE-221 85 Lund, Sweden.

* These authors contributed equally to this study

Address correspondence to:

Jonas Frisén, Phone +46 8 52487562, Fax +46 8 324927, e-mail jonas.frisen@ki.se

ABSTRACT

It has been difficult to establish whether we are limited to the heart muscle cells we are born with or if cardiomyocytes are generated also later in life. We have taken advantage of the integration of ^{14}C, generated by nuclear bomb tests during the Cold War, into DNA to establish the age of cardiomyocytes in humans. We report that cardiomyocytes renew, with a gradual decrease from 1% turning over annually at the age of 20 to 0.3% at the age of 75. Less than 50% of cardiomyocytes are exchanged during a normal lifespan. The capacity to generate cardiomyocytes in the adult human heart suggests that it may be rational to work towards the development of therapeutic strategies aiming to stimulate this process in cardiac pathologies.

Myocardial damage often results in chronic heart failure due to loss and insufficient regeneration of cardiomyocytes. This has prompted efforts to devise cardiomyocyte replacement therapies by cell transplantation or by the promotion of endogenous regenerative processes. The development of cell transplantation strategies is advancing fast and some are currently being evaluated in clinical trials (*1, 2*). Stimulating endogenous regenerative processes is attractive as it potentially could provide a non-invasive therapy and circumvent the immunosuppression required for allografts. However, it is unclear whether such regenerative strategies are realistic as it has been difficult to establish whether cardiomyocytes can be generated after the perinatal period in humans.

Stem/progenitor cells with the potential to generate cardiomyocytes in vitro remain in the adult rodent and human myocardium (*3, 4*). Moreover, mature cardiomyocytes have been suggested to be able to reenter the cell cycle and duplicate (*5*). However, studies over several decades in rodents using labeled nucleotide analogues have lead to conflicting results ranging from no to substantial generation of cardiomyocytes postnatally (*6*). A recent genetic labeling study, which enabled detection of cardiomyocyte generation by stem/progenitor cells (but not by cardiomyocyte duplication), demonstrated cardiomyocyte renewal after myocardial injury, but not during one year in the healthy mouse (*7*).

It is possible that humans, who live much longer than rodents, may have a different requirement for cardiomyocyte replacement. Cell turnover has been difficult to study in humans since the use of labeled nucleotide analogues and other strategies commonly used

in experimental animals cannot readily be adapted for studies in humans due to safety concerns. The limited functional recovery after loss of myocardium and the fact that primary cardiac tumours are very rare, indicate limited proliferation within the adult human heart (*8*). Several studies have described the presence of molecular markers associated with mitosis in the human myocardium (*5*), but this provides limited information as it is difficult to deduce the future fate of a potentially dividing cell in terms of differentiation and long-term survival.

We have measured ^{14}C from nuclear bomb tests in genomic DNA of human myocardial cells, which allows retrospective birth dating (*9-11*). ^{14}C levels in the atmosphere remained relatively stable until the Cold War when above ground nuclear bomb tests caused a dramatic increase (*12, 13*). Even though the detonations were conducted at a limited number of locations, the elevated ^{14}C levels in the atmosphere rapidly equalized around the globe as $^{14}CO_2$. After the Test-Ban Treaty in 1963, the ^{14}C levels have dropped exponentially, not primarily because of radioactive decay (half-life 5730 years), but by diffusion from the atmosphere (*14*). Newly created atmospheric ^{14}C reacts with oxygen to form $^{14}CO_2$, which is incorporated by plants through photosynthesis. By eating plants, and animals that live off plants, the ^{14}C concentration in the human body mirrors that in the atmosphere at any given point in time (*15-18*). Since DNA is stable after a cell has gone through its last cell division, the ^{14}C level in DNA serves as a date mark for when a cell was born and can be used to retrospectively birth date cells in humans (*9-11*).

We first carbon dated left ventricle myocardial cells, including cardiomyocytes and other cell types, to determine the extent of postnatal DNA synthesis in the human heart. DNA was extracted and ^{14}C levels measured by accelerator mass spectrometry (see table S1

and S2 for ^{14}C values and associated data). The cellular birth dates can be inferred from determining at what time the sample's ^{14}C level corresponded to the atmospheric levels (Fig. 1A). ^{14}C levels from all individuals born around or after the nuclear bomb tests corresponded to atmospheric levels several years after the subjects' birth (Fig. 1B), indicating substantial postnatal DNA synthesis. Analysis of individuals born before the period of nuclear bomb tests allows for sensitive detection of any turnover after 1955, due to the dramatic increase in ^{14}C levels. By analyzing individuals born at different time points prior to 1955 it is possible to establish up to which age DNA synthesis occurs, or whether it continues beyond that age. In all studied cases, born up to 22 years before the onset of the nuclear bomb tests, ^{14}C concentrations were elevated compared to the pre-nuclear bomb test levels (Fig. 1C). Thus, DNA is synthesized many years after birth, indicating that cells in the human heart do renew into adulthood.

Since cardiomyocytes comprise only about 20% of all cells within the human myocardium (*19*), it is not possible to infer from this data whether there is postnatal renewal of cardiomyocytes, or whether cell turnover in the myocardium is limited to other cell populations. We therefore set out to specifically birth date cardiomyocytes. Many cardiomyocytes are binucleated and it is difficult to distinguish a binucleated cell from two aggregating mononucleated cells (of which one could be a non-cardiomyocyte) in the flow cytometer. Hence, rather than separating myocardial cells based on cell surface or cytoplasmic markers, we developed a strategy to isolate cardiomyocyte nuclei by flow cytometry.

We found that the well characterized cardiomyocyte specific proteins cardiac troponin I (cTroponin I, also known as TNNI3) and cardiac troponin T (cTroponin T, also known as

TNNT2) (for review see (*20*)) have evolutionarily conserved nuclear localization signals and are partly localized in the nuclei of cardiomyocytes (fig. S1 and S2). Antibodies to cTroponin I and T identify the same subpopulation of nuclei in the myocardium (Fig. 2, A to D) and retrospective birth dating of nuclei isolated with antibodies against either epitope gave similar results (table S1). Western blot and qRT-PCR analysis of sorted nuclei demonstrated a high enrichment of cTroponin I and T in the positive fraction and a depletion in the negative, validating the efficiency of the strategy (Fig. 2, E to H and data not shown). We assessed the potential transfer of cTroponin I and T during tissue processing by mixing cardiac tissue with another tissue devoid of these proteins, and found that there was negligible transfer of cTroponin I or T to non-cardiomyocyte nuclei during tissue dissociation, nuclear preparation or flow cytometric sorting (fig. S2)**.**

We assessed the specificity of the isolation procedure with known cardiomyocyte-specific markers and markers of non-cardiomyocytes present in the myocardium. There was a high enrichment of nuclei containing the known cardiomyocyte-specific nuclear markers Nkx2.5 and GATA4 in the cTroponin positive fraction, with little contamination of nuclei expressing markers for fibroblasts, smooth muscle cells, endothelial cells or hematopoietic cells (Fig. 2, F to H and data not shown). Conversely, cardiomyocyte markers were depleted in the cTroponin negative fraction (Fig. 2, F to H and data not shown), indicating that close to all cardiomyocytes were isolated in the positive fraction. Sorting whole cells with antibodies to a non-nuclear cardiomyocyte specific epitope confirmed that nuclear cTroponin I and T are specific to cardiomyocytes, but resulted in lower purity compared to sorting nuclei (fig. S3). Flow cytometric reanalysis of all sorted samples demonstrated a DNA content corrected cardiomyocyte purity of 96±1.8% (mean

±SD, table S1 and fig. S4). Thus, flow cytometry with antibodies against cTroponin I or T allows specific isolation of cardiomyocyte and non-cardiomyocyte nuclei.

We extracted DNA from cardiomyocyte nuclei ($5\pm2x10^7$, mean±SD, table S1) and measured the ^{14}C concentration in genomic DNA. By analyzing the ^{14}C concentration also in unsorted myocardial nuclei ($>10^8$), we were able to mathematically compensate for any contamination in the cardiomyocyte fraction in the individual cases, reducing the risk that contamination with a cell population with a different turnover rate would skew the result for cardiomyocytes. All individuals born before the onset of the nuclear bomb tests had ^{14}C levels in cardiomyocyte genomic DNA that was higher than the pre-bomb atmospheric levels, demonstrating DNA synthesis after 1955 (Fig. 3A). Similarly, all individuals born near or after the time of the nuclear bomb tests had ^{14}C concentrations in cardiomyocyte DNA corresponding to several years after their birth, establishing postnatal cardiomyocyte DNA synthesis (Fig. 3B).

There is no increase in the number of cardiomyocytes after the postnatal period but rather a slow continuous decrease with age (*21*). About 25% of cardiomyocytes are binucleated in humans at birth, and this proportion stays constant throughout life (*22*). Thus, the postnatal cardiomyocyte DNA synthesis detected by ^{14}C analysis cannot be explained by an increase in cardiomyocyte number or binucleation. However, the heart grows during childhood, as the increasing demand of contractile capacity is met by hypertrophy of cardiomyocytes. Almost all cardiomyocyte nuclei are diploid at the time of birth, but the DNA of most nuclei is duplicated to become tetraploid in childhood when the cells undergo hypertrophy (Fig. 3C, fig. S5, (*23-25*)). After the age of ten there is no further increase in cardiomyocyte nuclei DNA content ($R=0.135$, $p=0.384$, Fig. 3C). The DNA

synthesis associated with polyploidization of cardiomyocyte DNA results in incorporation of ^{14}C concentrations corresponding to the atmospheric levels during childhood.

Three of the individuals born before the nuclear bomb tests were more than 10 years old at the onset of the increase in atmospheric ^{14}C. That their ^{14}C concentration in cardiomyocyte DNA was above the pre-nuclear bomb test levels (Fig. 3A) cannot be explained by DNA synthesis associated with polyploidization, but indicates cardiomyocyte renewal after 1955. Moreover, in the individuals born after the nuclear bomb tests the difference between the birth date of the person and the date corresponding to the ^{14}C level in cardiomyocyte DNA increased with the age of the individual (fig. S6, table S1), demonstrating that cardiomyocyte DNA synthesis is not restricted to a limited period in childhood but continues in adulthood.

Polyploidization of cardiomyocyte DNA occurs in a stereotypical manner during a rather short period in childhood (Fig. 3C, (*23-25*)), making it possible to calculate its impact on ^{14}C values in each individual (see supporting online text and (*26*)). By subtracting the childhood polyploidization-associated ^{14}C incorporation from the measured value in each case, we could estimate polyploidization-independent ^{14}C values. In all cases, the polyploidization-independent ^{14}C values corresponded to time points after birth for each individual (Fig. 3D), indicating cardiomyocyte renewal. Analysis of ^{14}C concentrations in DNA from only diploid or only polyploid cardiomyocyte nuclei demonstrated similar degrees of ^{14}C integration after childhood in both compartments, providing direct evidence for cardiomyocyte renewal independently of polyploidization and indicating similar turnover of diploid and polyploid cells (see supporting online text, fig. S7 and

table S3). In the five oldest individuals, who all were born before or at the onset of the nuclear bomb tests, the ^{14}C values were lower than contemporary values (Fig. 3D), establishing that not all cardiomyocytes had been exchanged after 1955 but that a substantial fraction remains from early in life even in the elderly.

Increased cardiac workload in pathological situations often results in cardiomyocyte hypertrophy and heart enlargement, and can at late stages result in polyploidization in adulthood (fig. S5, *24*). A few of the included subjects had cardiac pathology (table S2). We cannot exclude the possibility that adult polyploidization may contribute to some ^{14}C integration in the cases with pathology. However, none of the included subjects had severe heart enlargement nor a pathological cardiomyocyte ploidy profile and there was no significant difference in ^{14}C integration in cardiomyocyte DNA in the subjects with cardiac pathology compared to healthy individuals (table S1, Fig. 3C and fig. S5). Moreover, mathematical modeling of the kinetics of DNA synthesis and ^{14}C integration showed that the measured ^{14}C concentrations in cardiomyocyte DNA could not be a result of polyploidization during adulthood (see supporting online text).

Several studies of sex-mismatched transplant recipients have indicated fusion of human cardiomyocytes with other cells (*27*). However, fusion appears to mainly occur transiently after transplantation and even in the acute phase the fusion rate is too low to explain the ^{14}C data (fig. S8). DNA damage and repair is very limited in differentiated cells (*28*) and is, at least in neurons, well below the detection limit of the employed method (*10, 11*). Although cell fusion and DNA repair may affect ^{14}C levels in cardiomyocyte DNA, available data suggest that the magnitude of these processes make them negligible in the current context and that the ^{14}C data we report here (after

compensation for polyploidization) likely accurately reflects cell renewal.

Mathematical modeling of ^{14}C data from individuals born both before and after the nuclear bomb tests, which provides slightly different and complementary information, as well as of subjects of different age within these groups can provide an integrated view on cell turnover (*9*). We used an analytical model that includes polyploidization in childhood to assess which one of many scenarios for cell birth and death best describes the data. Times at which cells are born, ploidize and die are tracked. The atmospheric ^{14}C values corresponding to DNA synthesis events are integrated to yield a calculated ^{14}C level, based on each subject's birth date, age at death and DNA content. The calculated ^{14}C levels were fitted to the purity-corrected values to find the best renewal rates for each scenario (see supporting online text for a comprehensive description of the modeling). We first calculated what the annual turnover rate would be in each individual if the rate was constant throughout life. This indicated annual turnover rates of 0.2-2% (Fig. 4A). However, there was a clear negative correlation to age ($R=-0.85$; $p=0.005$), establishing that the turnover rate declines with age. The strong negative correlation to age also indicates that there is limited interindividual variation in the cardiomyocyte turnover rate and its decrease with age.

We next tested a series of different models allowing turnover rates to change with age. The best fit was found with an inverse-linear declining turnover rate (Fig. 4B), where younger cardiomyocytes were more likely than old to be replaced (see supporting online text). This model predicts that cardiomyocytes are renewed at a rate of approximately 1% per year at the age of 20 and 0.3% at the age of 75 (Fig. 4B). With this turnover rate, the majority of cardiomyocytes will never be exchanged during a normal lifespan (Fig. 4C).

At the age of 50, 60% of the cardiomyocytes remain from the time around birth and 40% have been generated later (Fig. 4C). The age of cardiomyocytes is in average 6 years younger than the individual (Fig. 4D). The ^{14}C data indicate a substantially higher renewal rate for non-cardiomyocytes, with a median annual turnover of 18% and a mean age of 4.0 years (see supporting online text). Our data does not allow us to identify whether new cardiomyocytes derive from cardiomyocyte duplication or from a stem/progenitor pool, as both would result in similar ^{14}C integration in DNA.

Analysis of cell proliferation in the human myocardium has previously indicated a cardiomyocyte proliferation rate that could result in the exchange of all cardiomyocytes within 5 years (*29*), but the ^{14}C concentrations in DNA exclude such a high mitotic renewal rate. We asked whether cardiomyocytes may be heterogeneous, with an identifiable subpopulation turning over relatively fast and the rest not turning over at all. This scenario is incompatible with the data, and it is most likely that the vast majority of cardiomyocytes have a similar probability to be exchanged at a given age (see supporting online text).

The limited functional recovery in humans after myocardial injury clearly demonstrates failing regeneration of cardiomyocytes. The renewal of cardiomyocytes indicated by the continuous integration of ^{14}C, suggests that the development of pharmacological strategies to stimulate this process may be a rational alternative or complement to cell transplantation strategies for cardiomyocyte replacement.

References and notes

1. R. Passier, L. W. van Laake, C. L. Mummery, *Nature* **453**, 322 (May 15, 2008).
2. M. A. Laflamme, C. E. Murry, *Nat Biotechnol* **23**, 845 (Jul, 2005).
3. S. Martin-Puig, Z. Wang, K. R. Chien, *Cell Stem Cell* **2**, 320 (Apr 10, 2008).
4. S. M. Wu, K. R. Chien, C. Mummery, *Cell* **132**, 537 (Feb 22, 2008).
5. P. Anversa, B. Nadal-Ginard, *Nature* **415**, 240 (Jan 10, 2002).
6. M. H. Soonpaa, L. J. Field, *Circulation research* **83**, 15 (Jul 13, 1998).
7. P. C. Hsieh *et al.*, *Nat Med* **13**, 970 (Sep, 2007).
8. J. Butany *et al.*, *Lancet Oncol* **6**, 219 (Apr, 2005).
9. K. L. Spalding *et al.*, *Nature* **453**, 783 (Jun 5, 2008).
10. R. D. Bhardwaj *et al.*, *Proc Natl Acad Sci U S A* **103**, 12564 (Aug 15, 2006).
11. K. Spalding, R. D. Bhardwaj, B. Buchholz, H. Druid, J. Frisén, *Cell* **122**, 133 (2005).
12. H. De Vries, *Science* **128**, 250 (Aug 1, 1958).
13. R. Nydal, K. Lovseth, *Nature* **206**, 1029 (Jun 5, 1965).
14. I. Levin, B. Kromer, *Radiocarbon* **46**, 1261 (2004).
15. K. L. Spalding, B. A. Buchholz, L.-E. Bergman, H. Druid, J. Frisén, *Nature* **437**, 333 (2005).
16. W. F. Libby, R. Berger, J. F. Mead, G. V. Alexander, J. F. Ross, *Science* **146**, 1170 (Nov 27, 1964).
17. D. D. Harkness, *Nature* **240**, 302 (Dec 1, 1972).
18. E. M. Wild *et al.*, *Nucl. Instr. and Meth. in Physics Res.* **172**, 944 (2000).
19. M. Rubart, L. J. Field, *Annu Rev Physiol* **68**, 29 (2006).
20. M. S. Parmacek, R. J. Solaro, *Progress in cardiovascular diseases* **47**, 159 (Nov-Dec, 2004).
21. G. Olivetti, M. Melissari, J. M. Capasso, P. Anversa, *Circulation research* **68**, 1560 (Jun, 1991).
22. G. Olivetti *et al.*, *Journal of molecular and cellular cardiology* **28**, 1463 (Jul, 1996).
23. V. Brodsky, D. S. Sarkisov, A. M. Arefyeva, N. W. Panova, I. G. Gvasava, *Virchows Arch* **424**, 429 (1994).
24. C. P. Adler, in *The development and regenerative potential of cardiac muscle,* J. O. Oberpriller, J. C. Oberpriller, A. Mauro, Eds. (Harwood academic publishers, New York, 1991), pp. 227-252.
25. P. Pfitzer, *Current Topics in Pathology* **54**, 125 (1971).
26. Materials and methods are availabe as supporting material on Science Online.
27. M. A. Laflamme, D. Myerson, J. E. Saffitz, C. E. Murry, *Circulation research* **90**, 634 (Apr 5, 2002).
28. T. Nouspikel, P. C. Hanawalt, *DNA Repair* **1**, 59 (2002).
29. A. P. Beltrami *et al.*, *N Engl J Med* **344**, 1750 (Jun 7, 2001).

30. We thank Richard Lee, Kirsty Spalding and members of the Frisén lab for valuable discussions, M. Toro and K. Hamrin for help with flow cytometry. Paula Reimer for assistance with radiocarbon interpretation, Robert Cassidy for technical advice, M. Stahlberg and T. Bergman for help with HPLC and D.

Kurdyla and P. Zermeno for producing graphite. This study was supported by grants from the Swedish heart-Lung Foundation, the Swedish Research Council, Knut och Alice Wallenbergs Stiftelse, Human Frontiers Science Program, the Swedish Cancer Society, the Foundation for Strategic Research, the Karolinska Institute, the Juvenile Diabetes Research Foundation, European Commission FP7 CardioCell and the Tobias Foundation. This work was performed in part under the auspices of the U.S. Department of Energy by Lawrence Livermore National Laboratory under contract DE-AC52-07NA27344. R.D.B. and F. B.-H. were supported by fellowship from the Canadian Institutes of Health Research.

Supporting Online Material

www.sciencemag.org

Materials and Methods

Figs. S1-S8

Tables S1 –S3

Supporting online text

FIGURE LEGENDS

Figure 1. Cell turnover in the heart

(A) Schematic figure demonstrating the strategy to establish cell age by ^{14}C dating. The black curve in all graphs shows the atmospheric levels of ^{14}C over the last decades (data from (*14*)). The vertical bar indicates the date of birth of the individual. The measured ^{14}C concentration (1) is related to the atmospheric ^{14}C level by using the established atmospheric ^{14}C bomb curve (2). The average birth-date of the population can be inferred by determining where the data point intersects the x-axis (3). ^{14}C levels in DNA of cells from the left ventricle myocardium in individuals born after (B) or before (C) the nuclear bomb tests correspond to time points substantially after the time of birth, indicating postnatal cell turnover. The vertical bar indicates the date of birth of each individual and the similarly colored dots represent the ^{14}C data for the same individual. For individuals born before the increase in ^{14}C levels, it is not possible to directly infer an age as the measured level can be a result of incorporation during the rising and/or falling part of the atmospheric curve, thus the level is indicated by a dotted horizontal line.

Figure 2. Isolation of cardiomyocyte nuclei

(A-C) Flow cytometric analysis of cardiomyocyte nuclei from the left ventricle of the human heart with an isotype control antibody or antibodies to the cardiomyocyte specific antigens cTroponin I or T. Boxes denote the boundaries for the positive and negative sort populations. (D) cTroponin I and T are present in the same subpopulation of heart cell nuclei. (E) Western blot analysis of flow cytometry-isolated nuclei demonstrates close to

all detectable cTroponin T (analyzed with two different antibodies) and I protein in the cTroponin T-positive fraction. Brain and heart tissue was used as negative and positive controls, respectively. (F) The cardiac troponin T-positive population is enriched for the cardiomyocyte-specific transcription factors Nkx2.5 and GATA4. Both fractions contain similar amounts of the nuclear protein histone 3 (loading control). (G) Gene expression analysis of flow cytometry-isolated nuclei shows a high expression level of cardiomyocyte specific genes in the cTroponin T-positive fraction (cTroponin I and T, Nkx2.5), while marker genes for endothelial cells (vWF), fibroblasts (vimentin), smooth muscle (ACTA2) and leukocytes (CD45) are highly expressed in the cTroponin T-negative fraction (H). Bars in (G, H) show the average from 3 independent experiments+-SD.

Figure 3. Cardiomyocyte turnover in adulthood

(A) The ^{14}C levels in cardiomyocyte DNA from individuals born before the time of the atmospheric radiocarbon increase correspond to time points after the birth of all individuals. The vertical bar indicates year of birth, with the correspondingly colored data point indicating the delta ^{14}C value. (B) ^{14}C levels in cardiomyocyte DNA from individuals born after the time of the nuclear bomb test. (C) Average DNA content (2n=100%) per cardiomyocyte nucleus from individuals (without severe heart enlargement, see figure S5) of different age. Ploidy was measured by flow cytometry. Colored data points identify individuals analyzed for ^{14}C (n=13). Black data points are from individuals only analyzed with regard to ploidy level (n=23) and white data points are taken from Adler et al. (n=26) (*24, 26*). The dashed lines indicate the 95% confidence

interval for the regression curve. (D) ^{14}C values corrected for the physiologically occurring polyploidization of cardiomyocytes during childhood for individuals born before and after the bomb spike, calculated based on the individual average DNA content per cardiomyocyte nucleus. The ^{14}C content is not affected in individuals where the polyploidization occurred before the increase in atmospheric levels.

Figure 4. Dynamics of cardiomyocyte turnover

(A) Individual data fitting assuming a constant turnover (see supporting online text) reveals an almost linear decline of cardiomyocyte turnover with age ($R=-0.85$; $p=0.005$). A constant turnover hypothesis might therefore not represent the turnover dynamics accurately. (B) Global fitting of all data points (see supporting online text, $SSE=9.4x10^3$) shows an age-dependent decline of cardiomyocyte turnover. (C) Fraction of cardiomyocytes remaining from birth is depicted as gray area, and the white area is the contribution of new cells. Estimation is from the best global fitting. (D) Cardiomyocyte age estimates from the best global fitting. The dotted line represents the no cell turnover scenario, where the average age of cardiomyocytes equals the age of the individual. The black line shows the best global fitting. Colored diamonds indicate computed data points from ^{14}C-dated subjects. Error bars in all graphs are calculated for each subject individually showing the interval of possible values fitted with the respective mathematical scenario.

Supporting online material

Materials and Methods

Tissue Collection

Tissues were procured from cases admitted during the period 2005-2007 to the Department of Forensic Medicine, Karolinska Institute, after receiving consent from relatives. Some heart samples were obtained from the UK Human Tissue Bank, Great Britain. Ethical permission for this study was granted by the Karolinska Institutet Ethical Committee. Human left ventricular tissue without the septum was dissected. Hearts were dissected and clotted blood was removed from the chambers before the heart weights were determined in accordance with the European Recommendation on the harmonization of medico-legal autopsy rules (*1, 2*). Then, epicardial fat and visible blood vessels were removed and the tissues were stored at –80 °C until analysis.

Nuclear Isolation

Left ventricular tissue (apex and wall) was thawed and whole-thickness samples were trimmed using a scalpel. Approximately 10g of tissue was added to 200mL of ice cold lysis buffer (0.32 M sucrose, 5 mM $CaCl_2$, 3mM magnesium acetate, 2.0 mM EDTA, 0.5 mM EGTA, 10 mM Tris-HCl (pH 8.0), 1 mM DDT) with a proteinase inhibitor cocktail (Sigma). All subsequent steps were performed on ice. The mixture was blended (Braun 600W blender) at speed turbo 9 for 10 minutes. The crude suspension was further homogenized by an Ultra-Turrax® homogenizer (IKA) at 20,000 rpm for 8 seconds. Triton X-100 was added to a final concentration of 0.2%, before the suspension was

dounced with a type A pestle exactly eight strokes in a glass douncer. The solution was put through a large filter sieve twice. Then, two layers of cotton gauze were placed on top of the sieve, and the solution was filtered two more times. This solution was consecutively filtered in 100 and 70 micron filters (Falcon) and equally divided into six 50 ml tubes. These tubes were centrifuged for 8 minutes at 1000g at 4 °C. The supernatant was carefully removed with a pipette from each tube and then discarded. The crude nuclear pellets were resuspended with 30 ml of 2.1 M sucrose solution (2.1 M sucrose, 3 mM magnesium acetate, 1 mM DTT, 10 mM Tris-HCl, pH 8.0). This was then layered onto a cushion of 10 ml 2.2 M sucrose solution (2.2 M sucrose, 3 mM magnesium acetate, 1 mM DTT, 10 mM Tris-HCl, pH 8.0), and centrifuged at 30,000g for one hour at 4°C. The supernatant was carefully pipetted off and discarded. The side of the tube was also carefully wiped to avoid supernatant contamination to the pellet. The pellet from each tube was then resuspended with 1,5 ml of nuclei buffer (0.43 M sucrose, 70 mM KCl, 2 mM MgCl2, 10 mM Tris-HCl (pH 7.2), 5 mM EGTA).

For the mixed heart/brain experiment, both tissue from the occipital cortex and left ventricle where processed together. Apart from an adjusted sucrose concentration of 2.0M, all procedures were performed as described above.

Flow Cytometry

Cardiomyocyte nuclei were isolated and collected using flow cytometry. A mouse monoclonal antibody to cTroponin I (Chemicon™, Millipore, MAB 3152), a polyclonal rabbit antibody to cTroponin T (Abcam, ab10224), or isotype control antibodies were directly conjugated to Alexa Fluor® 488 or 647 (Alexa Fluor® 488 or 647 Monoclonal

Antibody Labeling Kits, Molecular Probes™, Invitrogen). Antibodies to cTroponin T and cTroponin I were used at 1:800 to label cardiomyocyte nuclei, and left to incubate on ice for at least 30 minutes. Single nuclei (independent of their DNA content) were separated from doublets or higher-order aggregates by using a gating strategy using only physical parameters (*3*). Briefly, singlets were defined as a function of forward scatter width (FSC-W) and forward scatter height (FSC-H) which was defined based on the fluorescent intensity of the DNA stain DRAQ5®. All single nuclei, independent of their DNA content were detected within the defined gate (*4*), making it easy to discriminate singlets from doublets and other nuclei aggregates. All flowcytometric nuclei sorts were performed using the described sorting strategy.

For flow cytometry sorts of diploid and polyploidy cardiomyocyte nuclei and analysis of cardiomyocyte nuclei ploidy levels, nuclei were labeled with cTroponinT/I antibodies as described and DNA content was visualized with Hoechst33342 dye (5ug/ml) (Invitrogen, Molecular Probes®). Hoechst 33342 (5ug/ml) did not influence ^{14}C levels in cardiomyocyte DNA (n=5; p=0.69, Mann-Whitney test).

Purity of flowcytometrically sorted nuclei was confirmed by reanalyzing the sorted populations. ^{14}C levels were corrected if sorting purity was less than 100% (see Flow cytometry purity). For the mixed brain/heart experiment, we used the labeling protocol as described before (*3*). Brain tissue (occipital cortex) was homogenized together with left ventricular heart tissue. Nuclei were isolated as described before, incubated for 1-5h hours at 4°C and subsequently labeled with NeuN (Millipore, mab 377), cTroponinT and cTroponinI antibodies directly conjugated to Alexa® 488/647 dyes. All flowcytometric

experiments were performed by using a FACSVantage DiVa instrument (BD Bioscience).

Immunocytochemistry

Nuclear isolates were incubated for 30 min with an antibody to cTroponin T (1:800, Abcam, ab10224) or cTroponin I (1:800, Chemicon™, Millipore, MAB 3152) directly conjugated to Alexa Fluor® 488. Nuclei were counterstained with DAPI and transferred to slides. Pictures were taken with a Zeiss Meta® confocal microscope (Zeiss) and edited with Photoshop (Adobe®) software.

Gene expression of sorted nuclei.

Nuclei isolates were labeled with a cTroponin T antibody (Abcam, ab10224) and flow cytometric sorted according to their immunoreactivity. Total RNA was extracted from cTroponin T positive and negative populations (5-10 million nuclei), respectively, using the RNeasy mini plus kit (Qiagen). Equal amounts of total RNA from each sample was reverse transcribed to cDNA using the QuantiTect RT kit (Qiagen). In a final volume of 50 μL, 7.5 ng of cDNA was amplified with POWER SYBR PCR® master mix (Applied Biosystems) and primers (Eurofins MWG Operon). The primer pairs for cTroponin T (TNNT2), cTroponin I (TNNI3), Nkx2.5, vWF, vimentin, smooth muscle actin (ACTA2), CD45 and 28S ribosomal RNA (28S rRNA) were designed by using Primer3-BLAST ((*5*),NCBI, USA) and selected to yield a single amplicon based on dissociation curves. Quantitative real-time PCR was performed with a PRISM 7300 (Applied Biosystems). The relative mRNA levels were calculated using the C_t method, using 28S rRNA as a

normalizer. cTroponin T-positive nuclei served as a reference for TNNT2, TNNI3 and Nkx2.5. cTroponin T negative sorted nuclei served as a reference for vWF, vimentin, ACTA2 and CD45.

Western blot

Flow cytometry isolated nuclei ($1x10^6$) were spun down at $1.2x10^3$ g at 4°C for 15 minutes and lysed in RIPA lysis buffer (50 mM Tris, pH 7.2, 150 mM NaCl, 2 mM EDTA, 1% NP-40, 1% sodium deoxycholate, and 0.1% v/v SDS) supplemented with protease inhibitor cocktail (Roche) and separated by 10% or 12% SDS-PAGE. Equivalent amounts of whole human heart and brain tissues, or the heart cytoplasmic and nuclear fractions, were lysed in RIPA buffer. The proteins were transferred onto nitrocellulose membranes (Schleicher & Schuell) which were blocked in 5% milk and incubated at 4°C overnight with the following antibodies: cTroponin I (1:1000, mouse, Chemicon™, Millipore, MAB3152), cTroponin T (1:1000, rabbit, Abcam ab10224), cTroponin T 1:1000 (mouse, Abcam ab10214), Nkx 2.5 (1:500, mouse, R&D, MA2444), GATA4 (1:500, goat, R&D, AF2606), ERK1/2 (p44/p42 MAP kinase, 1:500, rabbit, Cell Signaling, 9102), αPAK (1:1000, rabbit, Santa Cruz (C-19)), TOM20 (1:5000, rabbit, Santa Cruz (FL-145)) or Histone3 (1:10 000, rabbit, Abcam, ab1791). Membranes were then incubated with the appropriate HRP-conjugated secondary antibody (1:2000; Amersham Biosciences,and Abcam) in 5% milk and detection was performed using ECL reagent and Hyperfilm (both from Amersham Biosciences).

Extraction of DNA

DNA extraction was performed as previously described (*6*). Briefly, isolated nuclei were suspended in 1 ml of 1% SDS, 5 mM EDTA-Na_2, 10 mM Tris-HCl, pH 8.0) and 8 µl of protease K solution (20 mg/ml, Invitrogen). The sample tube was then gently inverted numerous times and then incubated at 65°C overnight, with intermittent tube inversions. RNAse cocktail (8 µl, Ambion) was then added to each sample. Further 60 min incubation with inversions was then done. Three ml of a solution of sodium iodide (7.6 M NaI, 20 mM EDTA-Na_2, 40 mM Tris-HCl, pH 8.0) was then mixed to each sample followed by repeated inversion. Afterwards, 6 ml of filtered 99% ethanol was added and tubes gently inverted numerous times until the DNA precipitated. The DNA pellet was then washed in baths of 70% ethanol for 15 minutes for three times. Lastly, the DNA was rinsed in a water bath for 5 seconds, and then carefully transferred to a glass storage tube. The DNA pellet was resuspended in water after being thoroughly dried and then left to incubate up to seven days at 65°C, with many inversions, in order to completely dissolve the DNA into the water. The amount of DNA was quantified using spectrophotometry and only samples within a defined range (260/280: 1.8-2.0; 260/230: 2.0-2.4) were included into data analysis. In order to determine precisely remaining protein impurities all samples were additionally analyzed by means of HPLC. The mean protein contamination was 0.84%±0.17 SEM. Moreover, contamination by unidentified carbon sources can be detected by comparing the expected carbon content from the analyzed amount of DNA and the actual carbon content in the sample, which is measured in the accelerator mass spectrometry analysis. If a sample would contain more carbon than can

be accounted for by the DNA, this would mean that it was contaminated, but this was never the case.

Accelerator mass spectrometry

Accelerator mass spectrometry (AMS) analysis was performed blind to the identity of the sample. The DNA in water was moved to quartz AMS combustion tubes. They were then evaporated in a lyophilizer. Once completely dry, excess copper oxide (CuO) was introduced to each sample, the air was evacuated completely, and then sealed off with a H_2/O_2 torch. In order to completely combust all carbon to CO_2, these samples were then put into a 900°C furnace for 3.5 hours. The CO_2 that evolved during this process was then purified, trapped, and subsequently reduced to graphite in the presence of an iron catalyst in individual reactors (*7, 8*). CO_2 samples greater than 500 μg were split and the $\delta^{13}C$ measurement was attained by stable isotope ratio mass spectrometry. The graphite targets were then measured blindly at the Center for Accelerator Mass Spectrometry at Lawrence-Livermore National Laboratory, California, USA. A $\delta^{13}C$ correction of –23 +/- 2 was used for all samples (*9*). Background contamination corrections during the process of each AMS sample preparation were done according to the procedures of Brown and Southon (*10*). Each sample's measurement of error had values that ranged between ±2-10‰ (1 SD) $\Delta^{14}C$. Following the usual convention (*9*), all of the ^{14}C data are reported as decay corrected $\Delta^{14}C$ values since it is the most widespread for reporting post-bomb radiocarbon data (*9, 11*).

Bioinformatics

The following RefSeq sequences of human cTroponin T (TNNT2) and human cTroponin I (TNNI3) from NCBI were analyzed computationally for subcellular location. TNNT2: H. sapiens (NP_000355), M. musculus (AAH63753.1), G. gallus (NP_990780.1), closest D. melanogaster homologue by BLAST is upheld (NP_001014738.1; isoform F displayed highest number of NLS), C. elegans (NP_001024704.1). TNNI3: H. sapiens (NP_000354), M. musculus (NP_033432.1), G. gallus (NP_998735.1), D. melangogaster closest homologues wings up (NP_728141.1) and C. elegans (NP_507250.1).

Flow cytometry purity

In the case where sample purity of the cTroponin I-positive or cTroponin T-positive population was less than 100%, we corrected the measured ^{14}C levels applying the following equations. (*a*: purity of the cTroponin-positive population in %; *b*: measured ^{14}C value for the cTroponin-positve population; *c*: measured ^{14}C value for the unsorted population; *d*: ratio of cTroponin-positive nuclei in % (DNA weighted); *x*: purity corrected ^{14}C value for the cTroponin-positive population; *y*: purity corrected ^{14}C value for the cTroponin-negative population)

I $b*100 = x*a + y*(100-a)$ ***II*** $c*100 = x*d + y*(100-d)$

The equations were then solved for *x*.

III $x = (-100*c + c*a + 100*b - b*d)/(a-d)$

^{14}C value correction for polyploidisation

Nuclei isolates were incubated in Hoechst 33342 (5ug/ml) and DNA content was determined by flow cytometry (fig. S5A). The average DNA content per cardiomyocyte nuclei was calculated by establishing the arithmetic mean of the different ploidy levels (100% corresponds to a diploid population) in at least 10,000 cardiomyocyte nuclei of each analyzed heart sample. We also used published data of Adler on the ploidy distribution of children hearts to obtain the most comprehensive data collection (*12, 13*) (Fig. 3C).

An increase in the DNA content per nucleus during childhood leads to postnatal ^{14}C incorporation which is independent of cellular division. We used a computational approach to calculate polyploidisation independent delta ^{14}C values based on the atmospheric bomb curve and the polyploidisation time course in healthy individuals (Fig. 3D). In a first step, we calculated a regression curve that describes DNA content per nucleus with age f(a). We found that the sharp increase of DNA content around the age of six, can be best described by the following sigmoid curve with the parameters d_0=111.551, n=9.641, θ =6.773 and k=67.599 (R=0.955; SEE=10.149).

$$f(a) = d_0 H(a) + \frac{k}{1 + (\frac{a}{\theta})^{-n}}$$

No significant correlation after the age of ten between age and DNA content per nucleus is present during adulthood in healthy individuals (R=0.088, p=0.642) (Fig. 3C). In contrast to the stereotype time course of polyploidisation the individual adult DNA content per nucleus varies to a certain degree. Therefore we used the individual measured

DNA content per nucleus (DNA_i) to adjust ^{14}C values (C_{adj}) for polyploidisation (table S1). Value k dependent on adult DNA content is calculated as following and individual values of k are shown in the modeling supplement (supporting online text).

$$k = DNA_i - d_0$$

The change of DNA content can be described by the derivate of f: D(a) (see supporting online text for equation). For each subject of age a, at date t_{death} (born at calendar year t_{death}-a), the ^{14}C value was adjusted for polyploidisation ($C_{adj}(a)$).

$$C_{adj}(a) = \frac{\int_0^a K(t_{death} - a + s)\, D(s) ds}{\int_0^a D(s) ds}$$

The function K is the bomb curve (atmospheric ^{14}C levels). The denominator, the total DNA content at age a, is a normalization term.

The C_{adj} derived birthdate was determined for individuals born after the bomb spike (table S1). The age difference between the date of birth of the individual (DOB) and the C_{adj} derived birthdate was established. The obtained age difference was then subtracted from the average birth date of the cardiomyocytes population ($\Delta^{14}C$ derived birthdate), resulting in a ploidy independent average birth date of the cardiomyocyte population (Fig. 3D and table S1). For individuals born before the bomb-spike, ploidy independent ^{14}C values ($C_{independent}$) were calculated by subtracting the distance between the ^{14}C value at birth (C_{birth}) and the ploidy adjusted $\Delta^{14}C$ value (C_{adj}) from the measured $\Delta^{14}C$ value ($C_{measured}$) (Fig. 3D and table S1).

$$C_{independent} = C_{measured} - |C_{birth} - C_{adj}|$$

Human Ventricular Whole Cardiomyocyte Sorting

Human ventricular biopsy tissue was attained after consent to treatment and dissociated to single cell solution with Liberase Blendzyme 3 (0.1 mg/ml) (Roche Diagnostics), washed and spun down and resuspended in ice cold cardiomyocyte isolation buffer (130 mM NaCl; 5 mM KCl; 1.2 mM KH2PO4; 6 mM HEPES; 5 mM NaHCO3; 1 mM MgCl2; 5 mM Glucose). Cells were fixed with BD Cytofix/Cytoperm™ solution, permeabilised and incubated o/n at 4˚C with predetermined optimal concentrations of monoclonal antibodies to cardiac myosin heavy chain IgG1 □ (□- and β–MHC) (Abcam, ab15), □-smooth muscle actin IgG □ (□-SMA) (Abcam, ab32575) and CD31 IgG2a □ (Pecam-1) (eBioscience, 25-0311) in BD Perm / Wash™ Buffer in the dark on a shaker. Cells were washed and spun down twice and resuspended in secondary antibody cocktail containing predetermined optimal concentrations of donkey anti mouse Alexa Fluor® 488 (Molecular Probes™, Invitrogen A-21202) and donkey anti Rabbit Alexa Fluor® 647 (Molecular Probes™, Invitrogen A-31573), and appropriate isotype antibodies, in BD Perm / Wash™ buffer in the dark on a shaker at 4˚C for 3 hours. Cells were washed twice and resuspended in PBS and 5% FCS and then sorted on a BD FACSAria on low pressure with a 100□m nozzle.

Human Ventricular Cardiomyocyte Nuclei Isolation

Sorted cardiomyocytes were suspended in hypotonic buffer (0.01M Hepes and 1.5mM $MgCl_2$, pH 7.2) for 10 minutes on ice and then lysis buffer (3% glacial acetic acid and 5% ethylhexadecyldimethylammonium bromide in H_2O; Sigma) per 5ml of hyptonic buffer was added to washed cells, and tubes were shaken every minute for 10 minutes. The release of nuclei was examined by light microscopy. Nuclei were washed in nuclei wash

buffer (320 mM sucrose, 5 mM $MgCl_2$, 10 mM HEPES at pH 7.4) and spun down twice. Nuclei were then resupended in BD Perm / Wash™ buffer containing predetermined optimal concentrations of monoclonal mouse anti cTroponin I (Chemicon™, Millipore, MAB3152) and monoclonal cTroponin T (Neomarkers, Ab-1) Conjugated to Alexa Fluor® 647 with monoclonal antibody labeling kit (Molecular Probes™, Invitrogen A20186) for 3 hours in the dark on a shaker at 4˚C. Nuclei were washed in nuclei wash buffer and resupended in BD Perm / Wash™ buffer containing predetermined optimal concentration of donkey anti mouse Alexa Fluor® 488 (Molecular Probes™, Invitrogen A-21202) for 1.5 hours in the dark on a shaker at 4˚C. Appropriate isotype antibodies were also used. Nuclei were washed twice in nuclei wash buffer, resuspended in PBS passed through a 70□m filter and acquired on a BD FACSAria flowcytometer.

References and notes

1. G. L. de la Grandmaison, I. Clairand, M. Durigon, *Forensic Sci Int* **119**, 149 (Jun 15, 2001).
2. B. Brinkmann, *Int J Legal Med* **113**, 1 (1999).
3. K. L. Spalding, R. D. Bhardwaj, B. A. Buchholz, H. Druid, J. Frisen, *Cell* **122**, 133 (Jul 15, 2005).
4. R. P. Wersto *et al.*, *Cytometry* **46**, 296 (Oct 15, 2001).
5. S. Rozen, H. J. Skaletsky, in *Bioinformatics Methods and Protocols: Methods in Molecular Biology.,* K. S, M. S, Eds. (Humana Press, Totowa, NJ, 2000), pp. 365-386.
6. R. D. Bhardwaj *et al.*, *Proc Natl Acad Sci U S A* **103**, 12564 (Aug 15, 2006).
7. G. M. Santos, J. R. Southon, K. C. Druffel-Rodriguez, S. Griffin, M. Mazon, *Radiocarbon* **46**, 165 (2004).
8. J. S. Vogel, J. R. Southon, D. E. Nelson, *Nucl. Instrum. Methods Phys. Res. Sect. B* **29**, 50 (1987).

9. M. Stuiver, H. A. Polach, *Radiocarbon* **19**, 355 (1977).
10. T. A. Brown, J. R. Southon, *Nucl. Instrum. Methods Phys. Res. Sect. B* **123**, 208 (1997).
11. P. J. Reimer, T. A. Brown, R. W. Reimer, *Radiocarbon* **46**, (2004).
12. C. P. Adler, *Beitr Pathol* **158**, 173 (Jul, 1976).
13. C. P. Adler, in *The development and regenerative potential of cardiac muscle,* J. O. Oberpriller, J. C. Oberpriller, A. Mauro, Eds. (Harwood academic publishers, New York, 1991), pp. 227-252.

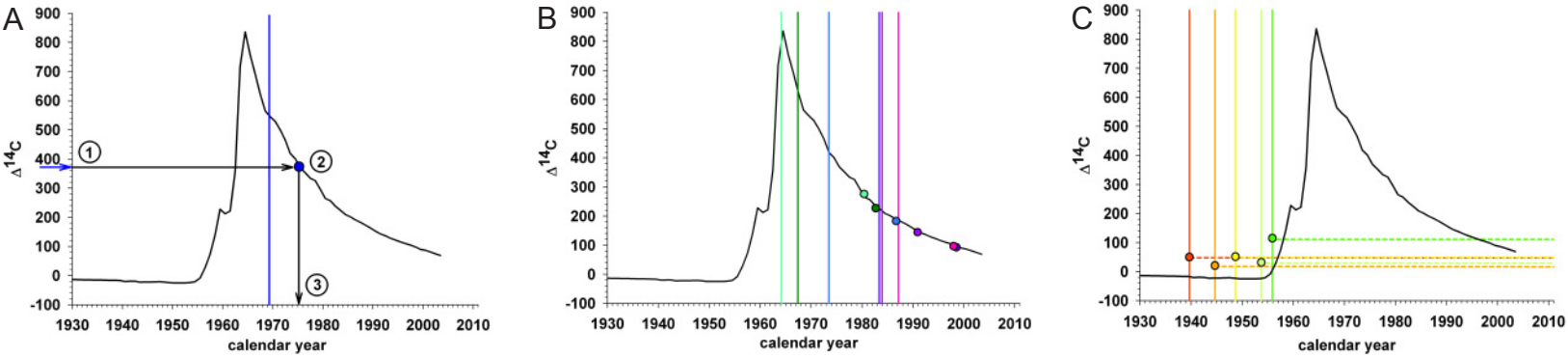
A
B
C
Δ14C
calendar year
900
800
700
600
500
400
300
200
100
0
-100
1930
1940
1950
1960
1970
1980
1990
2000
2010
1
2
3

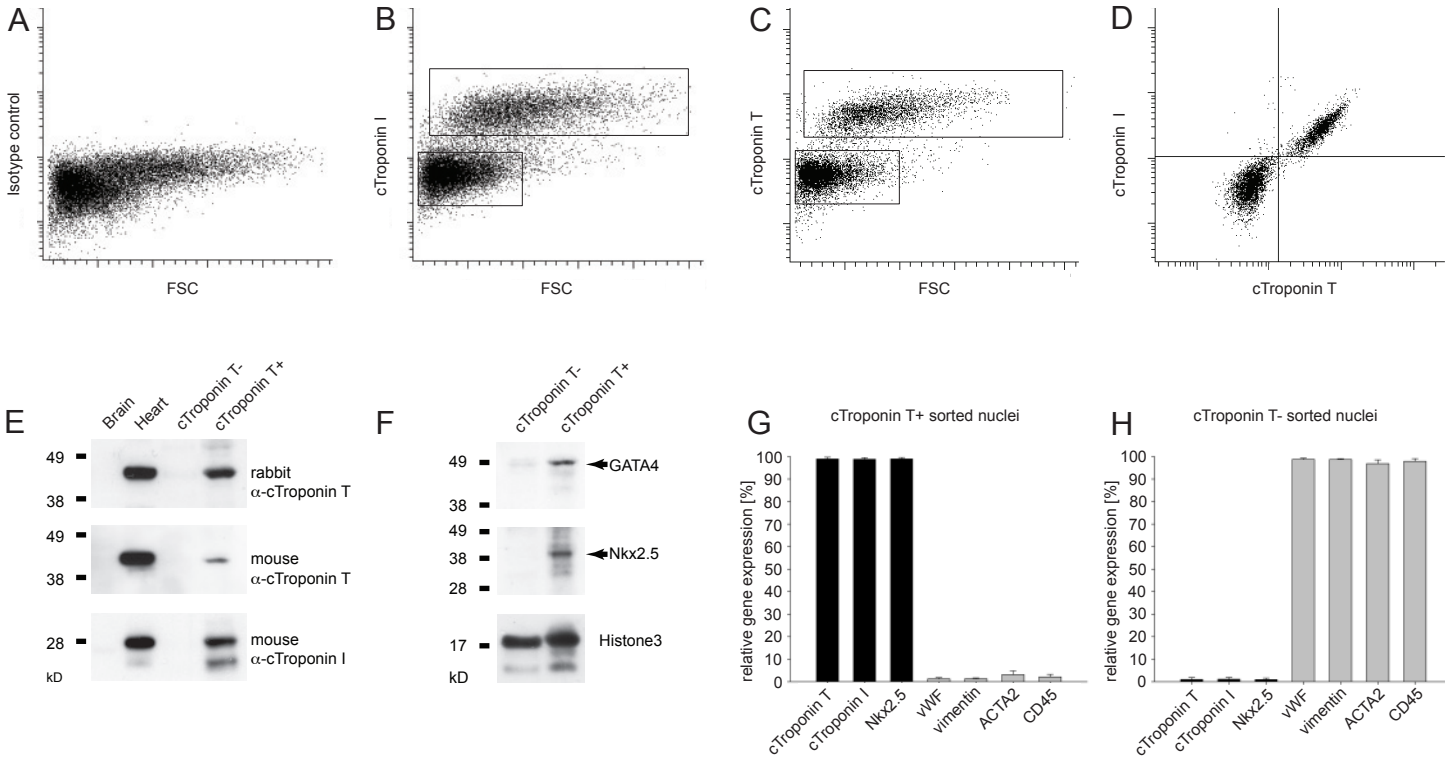
A
Isotype control
FSC
B
cTroponin I
FSC
C
cTroponin T
FSC
D
cTroponin I
cTroponin T
E
Brain
Heart
cTroponin T-
cTroponin T+
49
38
rabbit
α-cTroponin T
49
38
mouse
α-cTroponin T
28
mouse
α-cTroponin I
kD
F
cTroponin T-
cTroponin T+
49
38
GATA4
49
38
28
Nkx2.5
17
Histone3
kD
G
cTroponin T+ sorted nuclei
relative gene expression [%]
100
90
80
70
60
50
40
30
20
10
0
cTroponin T
cTroponin I
Nkx2.5
vWF
vimentin
ACTA2
CD45
H
cTroponin T- sorted nuclei
relative gene expression [%]
100
90
80
70
60
50
40
30
20
10
0
cTroponin T
cTroponin I
Nkx2.5
vWF
vimentin
ACTA2
CD45

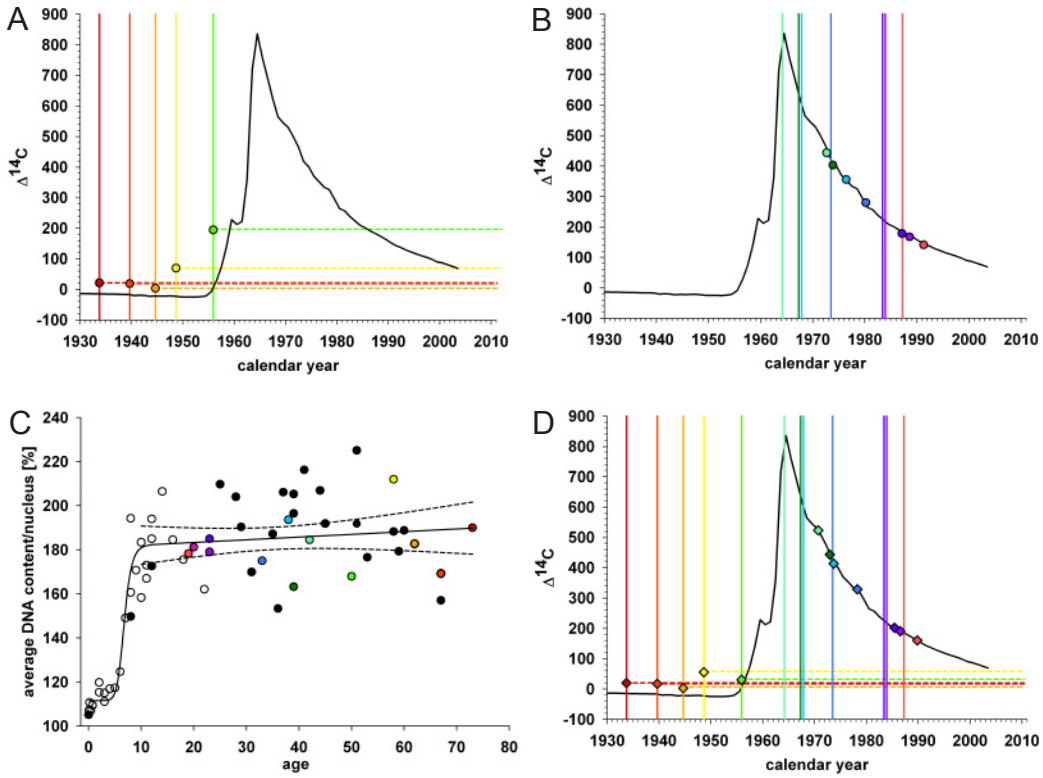
A
B
C
D
Δ14C
calendar year
average DNA content/nucleus [%]
age

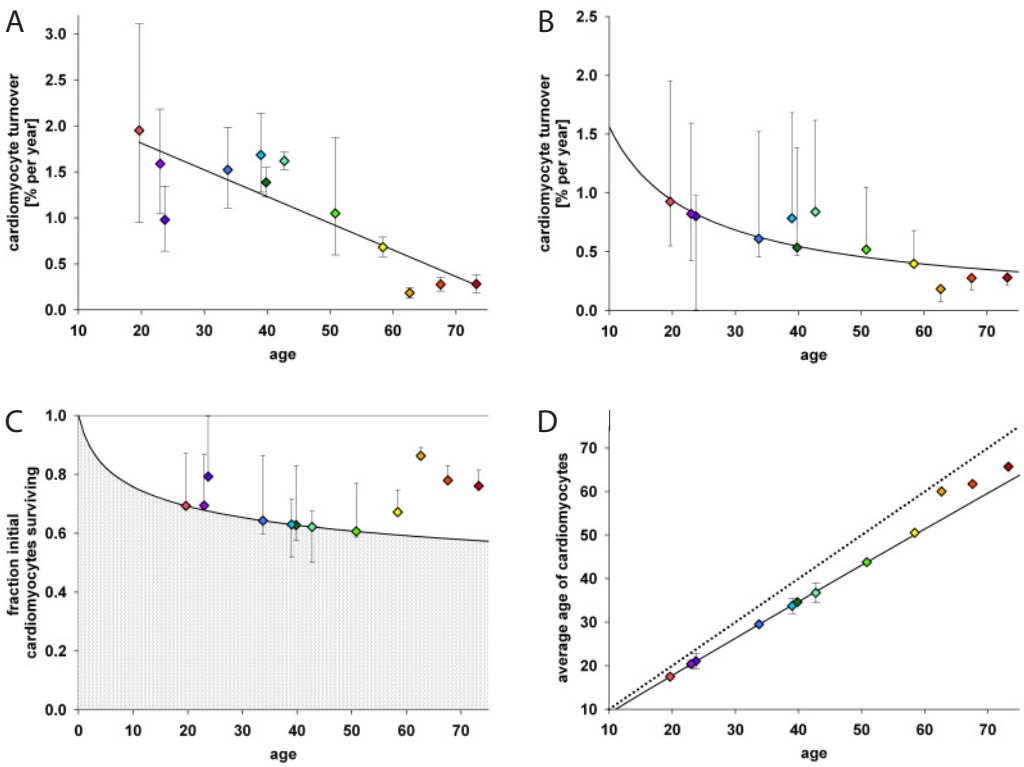
A
cardiomyocyte turnover [% per year]
age
B
cardiomyocyte turnover [% per year]
age
C
fraction initial cardiomyocytes surviving
age
D
average age of cardiomyocytes
age

A

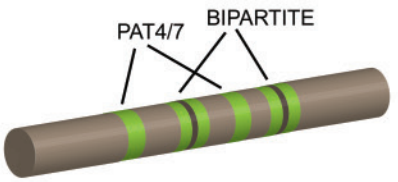

cardiac Troponin T
TNNT2

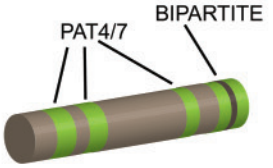

cardiac Troponin I
TNNI3

B

C

Protein	PSORT II NLS (Bipartite)	PSORT II %Nuclear	NucPred Score	Specificity
TNNT2 H. sapiens	4 (2)	73.9	0.87	0.84
Tnnt2 M. musculus	4 (2)	78.3	0.86	0.84
TNNT2 G. gallus	4 (3)	82.6	0.93	0.88
upheld (f) D. melanogaster	5 (4)	82.6	0.94	0.88
TNT-2 C. elegans	2 (1)	69.6	0.81	0.84
GATA-4 H. sapiens	1	82.6	0.64	0.71
MYL2 H. sapiens	1	8.7	0.11	0.45

Protein	PSORT II NLS (Bipartite)	PSORT II %Nuclear	NucPred Score	Specificity
TNNI3 H. sapiens	4 (1)	73.9	0.75	0.81
TNNI3 M. musculus	4 (1)	73.9	0.73	0.81
TNNI3 G. gallus	3 (2)	87.0	0.76	0.81
wings up D. melanogaster	3 (3)	78.3	0.71	0.81
Ce TNI-3 C. elegans	3 (3)	87.0	0.65	0.71
GATA-4 H. sapiens	1	82.6	0.64	0.71
MYL2 H. sapiens	1	8.7	0.11	0.45

Figure S1

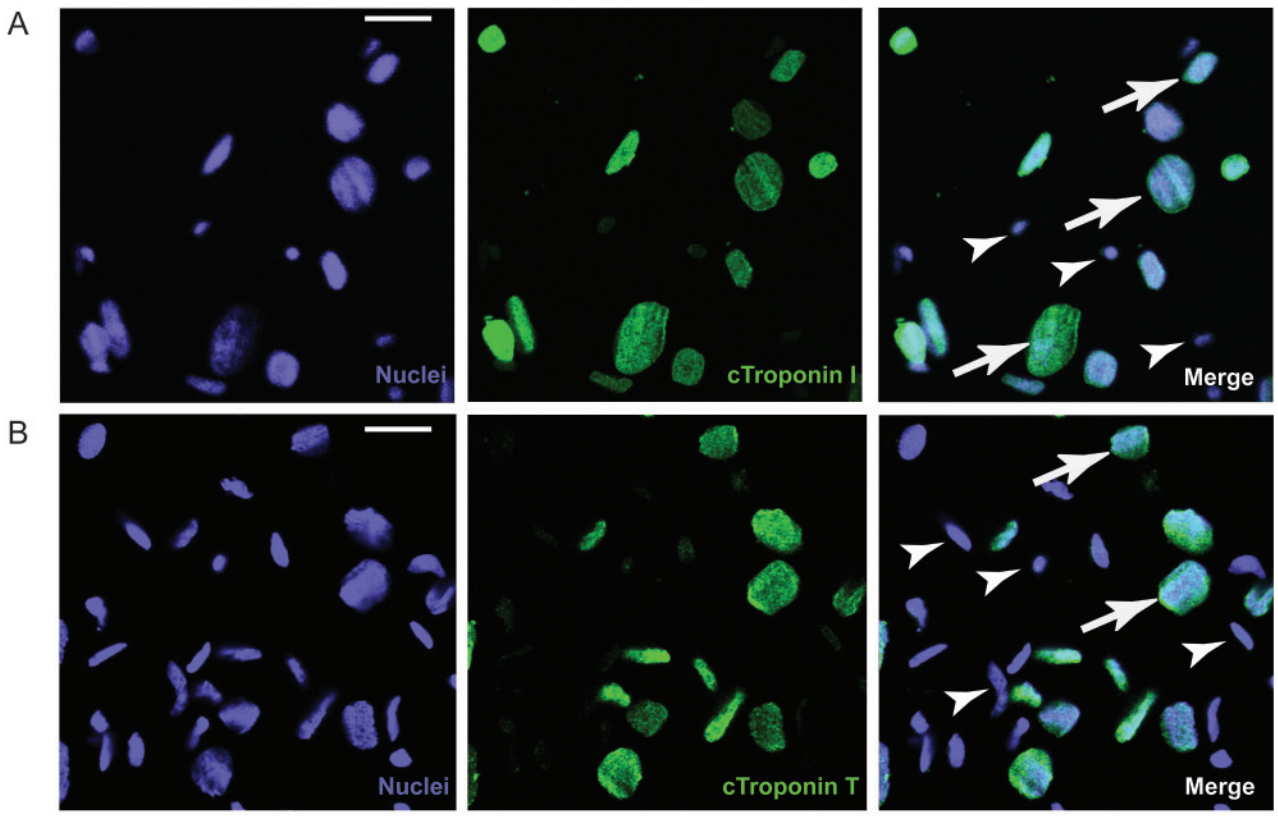
A
Nuclei
cTroponin I
Merge
B
Nuclei
cTroponin T
Merge

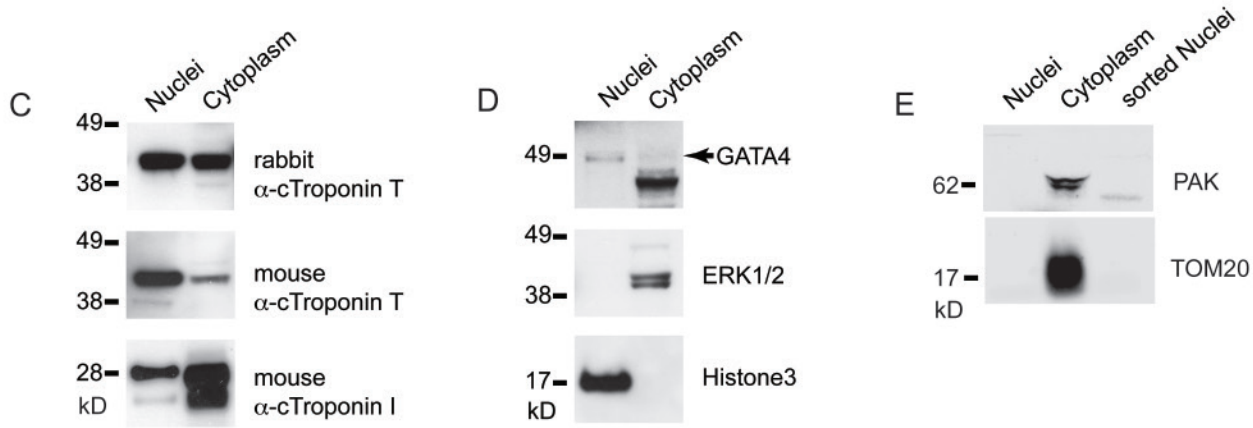
C
Nuclei
Cytoplasm
49
38
rabbit
α-cTroponin T
49
38
mouse
α-cTroponin T
28
kD
mouse
α-cTroponin I
D
Nuclei
Cytoplasm
49
GATA4
49
38
ERK1/2
17
kD
Histone3
E
Nuclei
Cytoplasm
sorted Nuclei
62
PAK
17
kD
TOM20

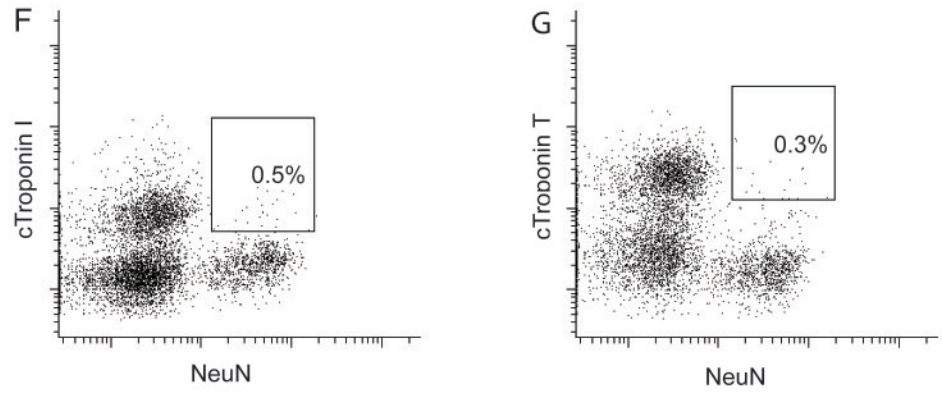
F
cTroponin I
0.5%
NeuN
G
cTroponin T
0.3%
NeuN

Figure S2

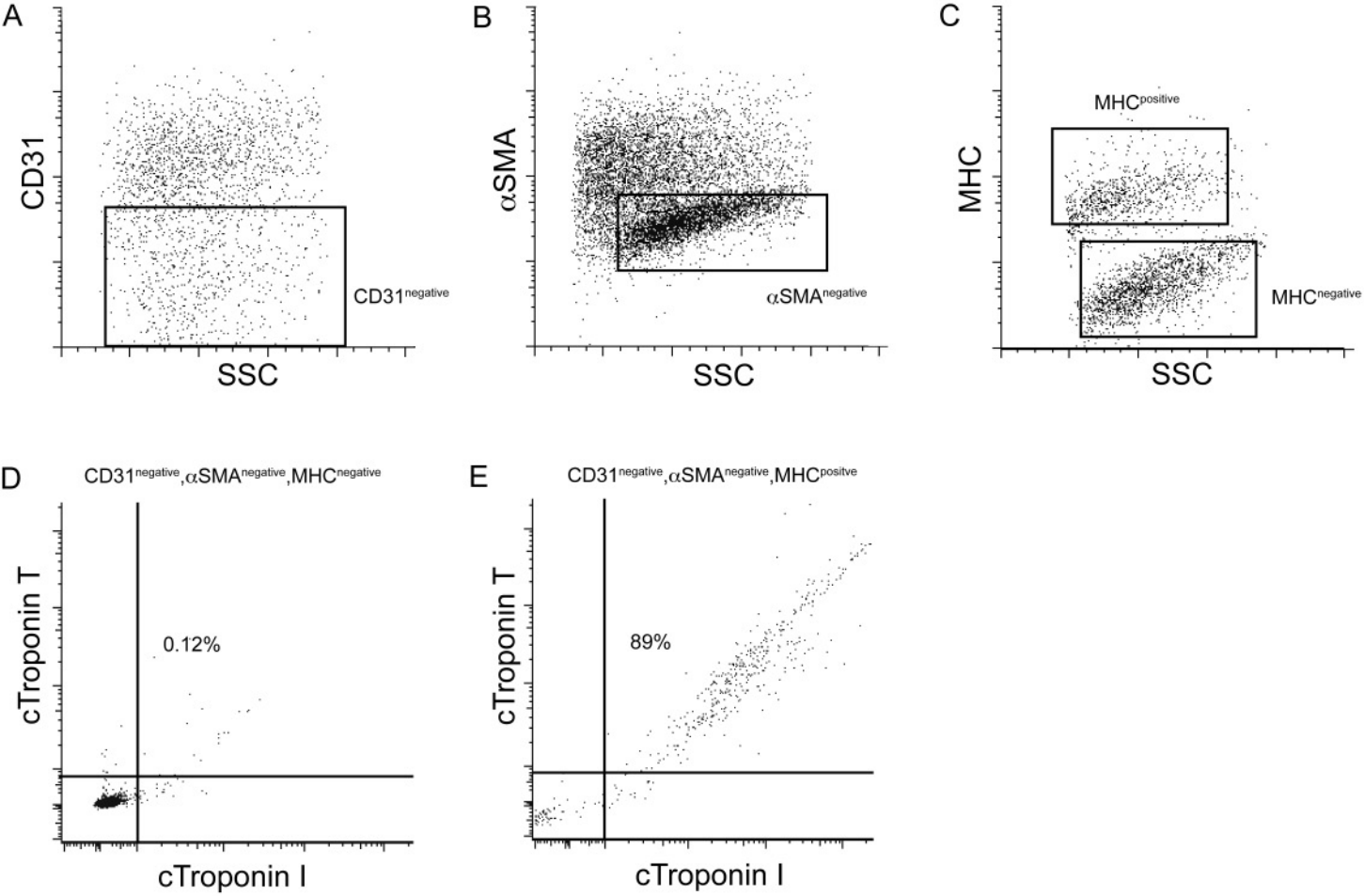
A
CD31
CD31negative
SSC
B
αSMA
αSMAnegative
SSC
C
MHCpositive
MHC
MHCnegative
SSC
D
CD31negative,αSMAnegative,MHCnegative
0.12%
cTroponin T
cTroponin I
E
CD31negative,αSMAnegative,MHCpositve
89%
cTroponin T
cTroponin I

Figure S3

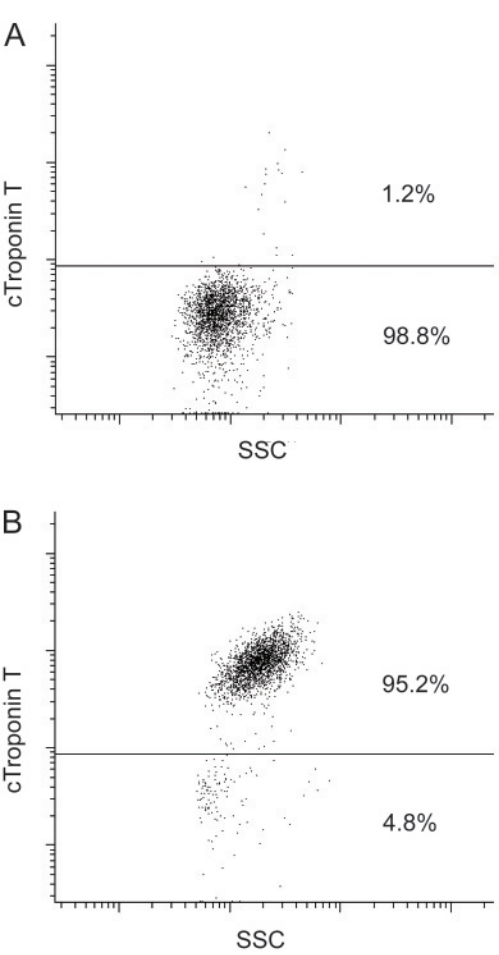

Figure S4

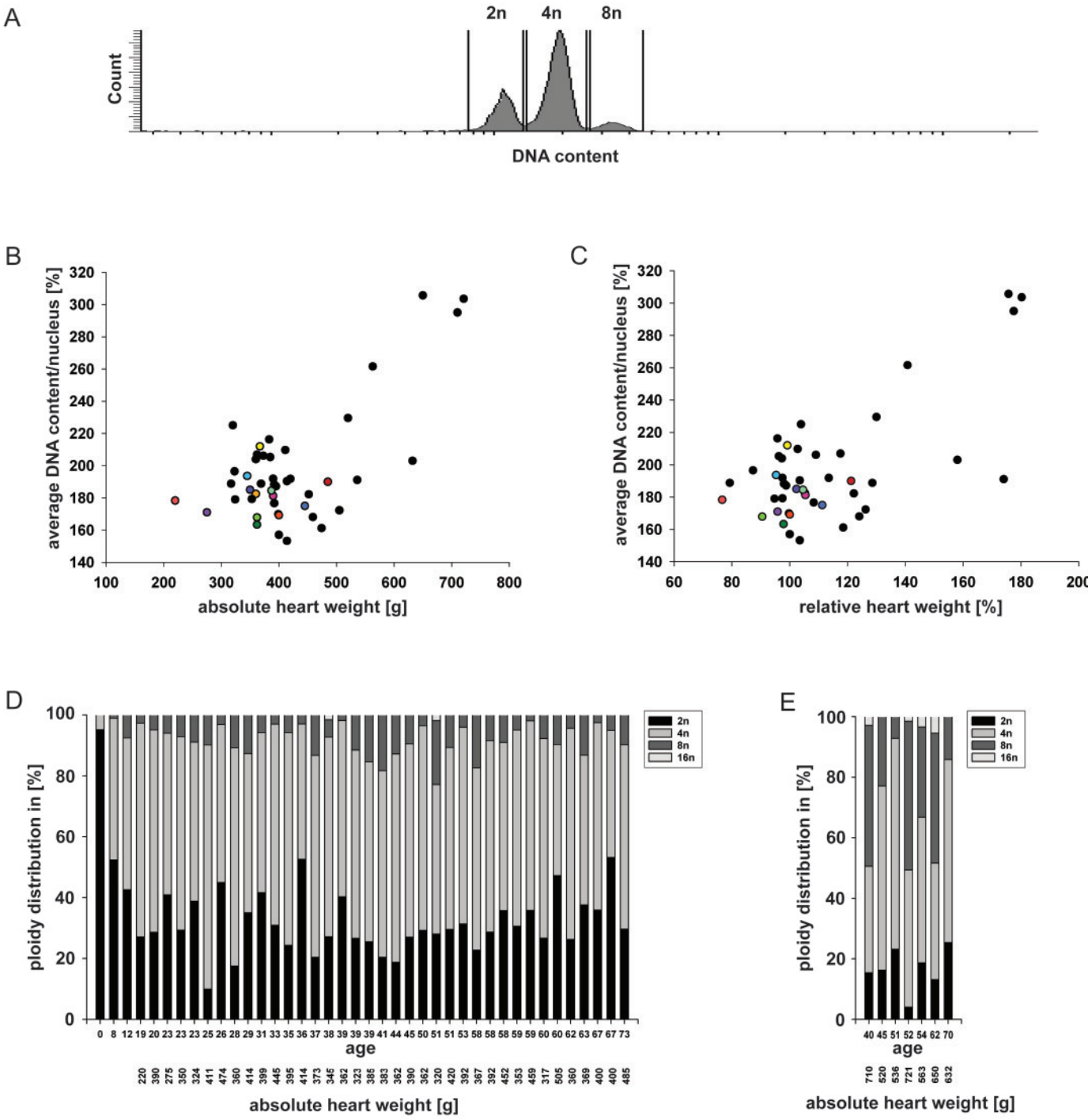
A
2n
4n
8n
Count
DNA content
B
average DNA content/nucleus [%]
absolute heart weight [g]
C
average DNA content/nucleus [%]
relative heart weight [%]
D
ploidy distribution in [%]
2n
4n
8n
16n
age
absolute heart weight [g]
E
ploidy distribution in [%]
2n
4n
8n
16n
age
absolute heart weight [g]

Figure S5

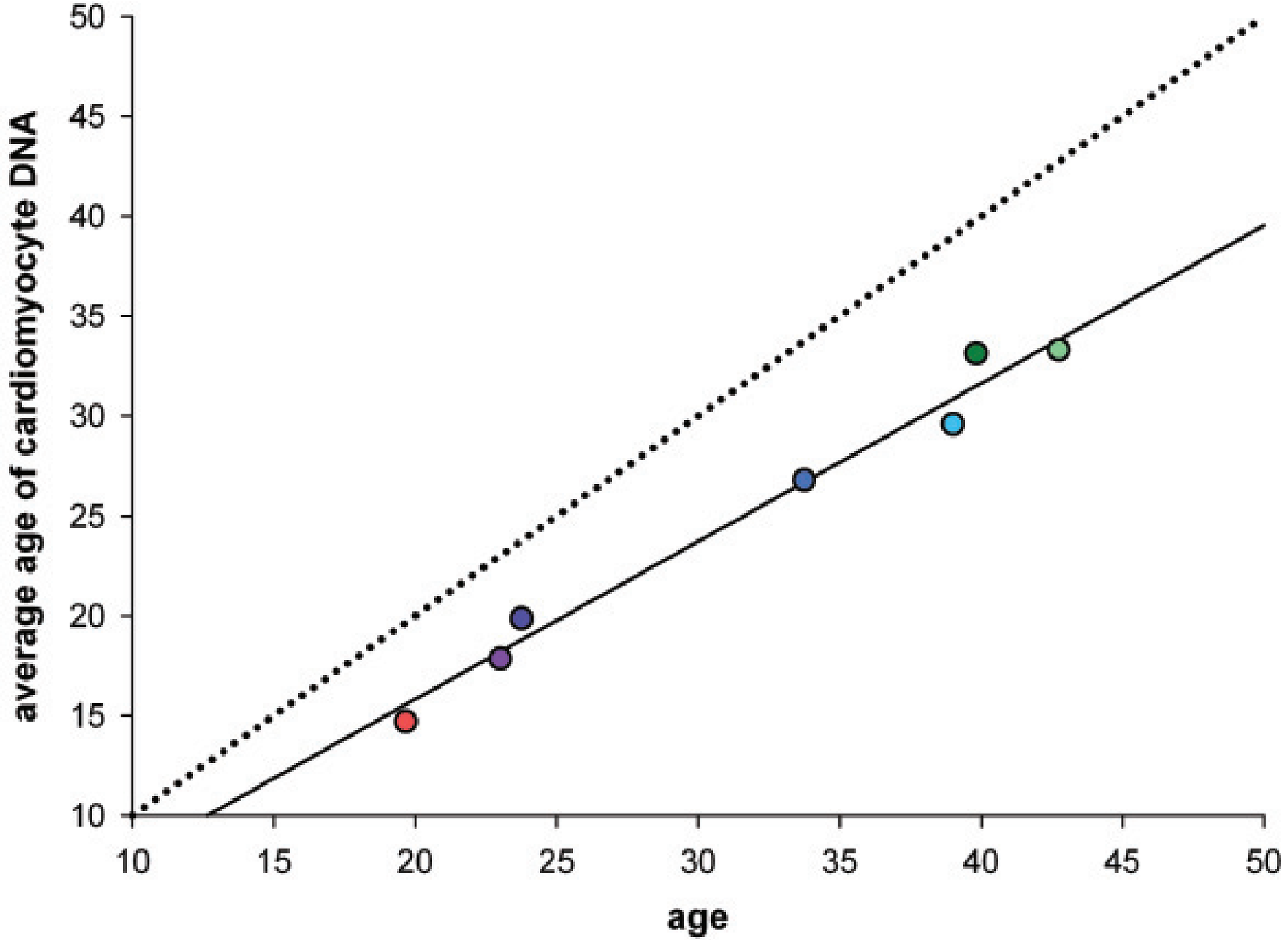
average age of cardiomyocyte DNA
50
45
40
35
30
25
20
15
10
10
15
20
25
30
35
40
45
50
age

Figure S6

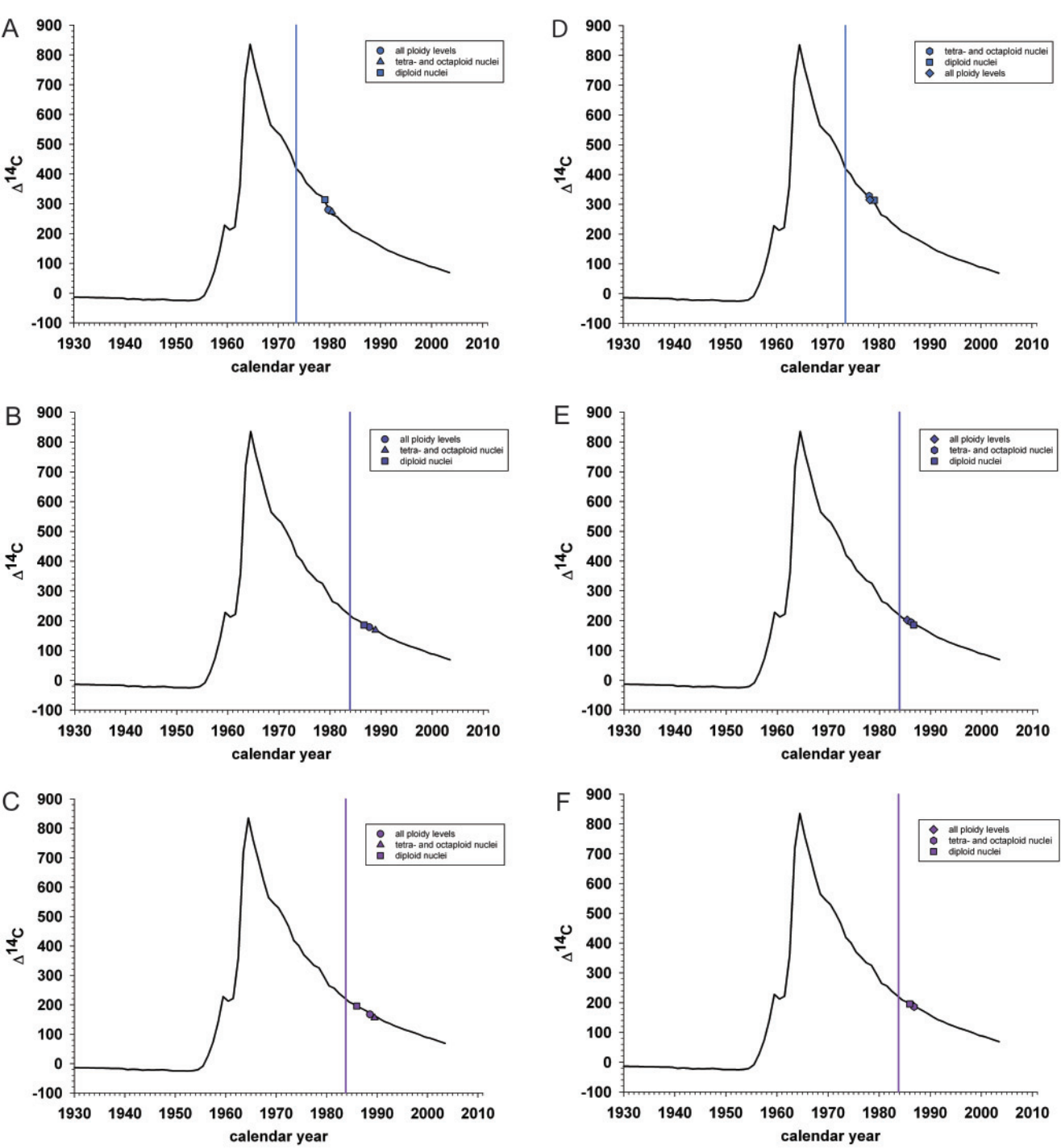
A
B
C
D
E
F
Δ14C
calendar year
all ploidy levels
tetra- and octaploid nuclei
diploid nuclei

Figure S7

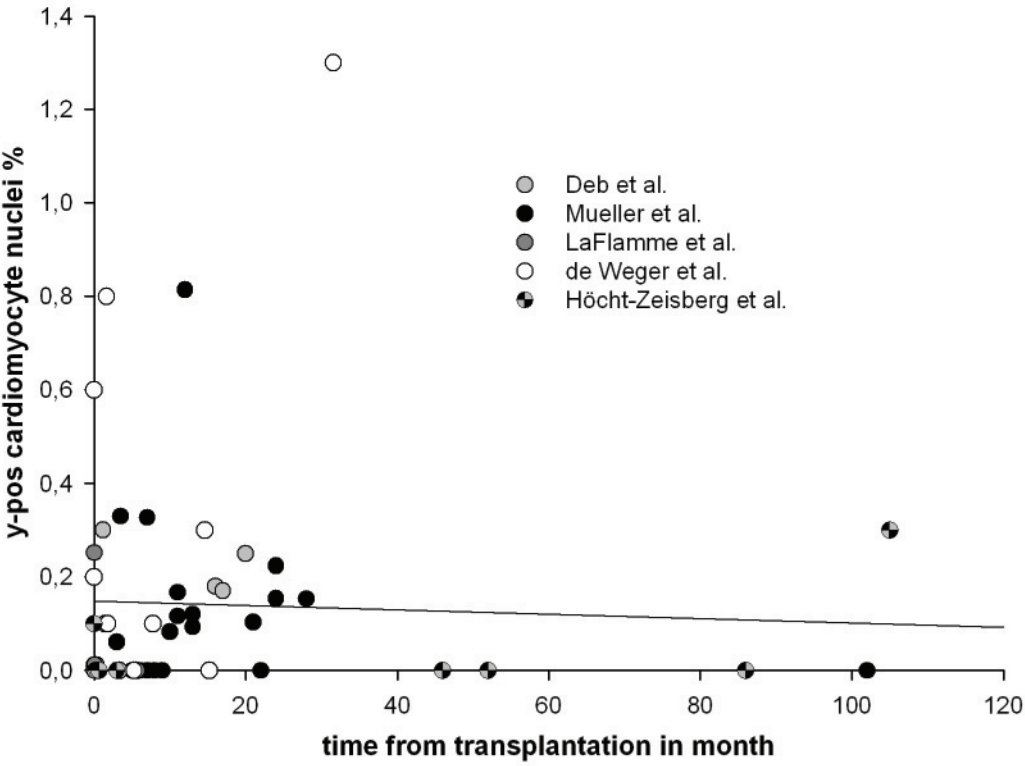
1,4
1,2
1,0
0,8
0,6
0,4
0,2
0,0
y-pos cardiomyocyte nuclei %
Deb et al.
Mueller et al.
LaFlamme et al.
de Weger et al.
Höcht-Zeisberg et al.
0
20
40
60
80
100
120
time from transplantation in month

Figure S8

Legends to Supporting Figures and Tables

Figure S1. Nuclear localization signals (NLS) within cTroponin T (TNNT2) and cTroponin I (TNNI3).

Since non-cardiomyocytes are very adherent to and are often in very close proximity to cardiomyocytes within the myocardium, a strategy based on cell sorting may not allow for the desired purity as it may be difficult to exclude cell doublets. Since a substantial proportion of cardiomyocytes are binucleate, it is not possible to avoid doublets by excluding cells with more than two nuclei. By choosing to sort for cardiomyocyte nuclei as opposed to whole cells, we could better control purification and still obtain the desired DNA.

(A) We took a bioinformatic approach to search for predicted nuclear localization signals within cytoplasmic cardiomyocyte markers. We found that cTroponin T (TNNT2) (left panel) and cTroponin I (TNNI3) (right panel) both contain four putative nuclear localization signals. **(B)** NucPred ClustalW alignment between species shows the relative basic residue content and distribution (positive=more likely nuclear). Species display a similar NLS organisation near the N-termini of the protein. **(C)** Table showing specifity for nuclear localization of cTroponin T and I for different species. Nuclear GATA4 (NP_002043.2) and cytosolic cardiac myosin light chain were used as positive and negative controls, respectively. Specificity represents the binned fraction of proteins predicted to be nuclear that have been experimentally confirmed (greater is more reliable).

Figure S2. cTroponin T and cTroponin I are both present in cardiomyocyte nuclei.

(A, B) To verify the nuclear localization, a nuclear isolate from left ventricular tissue was incubated with DAPI (which labels DNA and reveals all nuclei) and antibodies against cTroponin I **(A)** or cTroponin T **(B)**. cTroponin I and T-immunoreactivity was present in a subset of nuclei that were larger in size than the unlabeled nuclei. Arrows point to cTroponin I and cTroponin T-immunoreactive nuclei and arrowheads to negative nuclei. Scale bars are 20µm. **(C)** We next performed Western blot analyses to further characterize the cTroponin I and cTroponin T-immunoreactive epitopes in the nuclei. Analysis of heart tissue separated into a cytoplasmic and a nuclear fraction by centrifugation revealed the presence of cTroponin I (approx. 28 kDa and 25kDa) and cTroponin T (approx. 40 kDa) in the cytoplasm as well as in the nuclei (left panel). The two different cTroponin I bands have been suggested to represent different phosporylation states (*1, 2*). Interestingly, one kinase known to phosphorylate cTroponin I is the nuclear protein TNNI3K, in line with the presence of the putatively phosphorylated form in the nucleus (*3*). **(D, E)** ERK1/2 and PAK detection only in the cytoplasm, and GATA4 as well as Histone 3 detection only in the nuclei, confirmed the purity of both cellular fractions. **(E)** TOM20, a import receptor protein localized in the outer mitochondrial membrane, was highly enriched only in the cytoplasmic fraction, demonstrating little mitochondrial contamination both in the flow cytometry sorted nuclear fraction (third lane) and in the nuclear fraction purified by sucrose cushion (first lane). **(F, G)** To address whether transfer of free cTroponin I or T to nuclei may occur,

resulting in false positive labeling, we mixed brain and heart tissue and analyzed whether neuronal nuclei were labeled with antibodies against cTroponin I **(F)** and cTroponin T **(G)**. Since this protein is not expressed in the brain, labeling of neuronal nuclei would indicate the transfer of this protein to the nuclei. We did not find labeling of neuronal nuclei (NeuN-positive) above background levels (0.3-0.5%), arguing against transfer of cTroponin I or cTroponin T to noncardiomyocyte nuclei during the isolation strategy.

Figure S3. cTroponin T and cTroponin I are both present in adult cardiomyocyte nuclei in human heart tissue biopsies.

Human left ventricular cardiomyocytes were isolated from human bioptic heart tissue by means of flow cytometry. Cardiomyocytes were defined as $CD31^{negative}$ (**A**), □-$SMA^{negative}$ (**B**) and $MHC^{positive}$ (**C**) and sorted accordingly. Nuclei from the $CD31^{negative}$, □-$SMA^{negative}$, $MHC^{positive}$ population (cardiomyocytes) and $CD31^{negative}$, □-$SMA^{negative}$, $MHC^{negative}$ population (negative control) were extracted subsequentially and reanalyzed by flow cytometry. cTroponin I and cTroponin T were not detected above background level (0.12%) in non-cardiomyocyte nuclei (**D**) whereas 89% of all cardiomyocyte nuclei were positive for both cTroponins (**E**). Abbreviations: SMA=smooth muscle actin; MHC=cardiac myosin heavy chain.

Figure S4. Reanalysis of flow cytometric sorted myocardial nuclei.

(A) Representative flowcytometric plot depicting cTroponin T-negative fraction with a contamination of 1.2% cTroponin T-positve nuclei. **(B)** Re-analysis of flow cytometric sorted cTroponin T-positive fraction with a contamination of 4.8% of cTroponin T-

negative nuclei.

Figure S5. Flow cytometric analysis of DNA content in human cardiomyocyte nuclei. **(A)** Representative flowcytometric plot showing different DNA levels of sorted human cardiomyocyte nuclei. Nuclei were incubated with Hoechst33342 (5μg/ml) before analysis. Average DNA content per cardiomyocyte nucleus [%] in left ventricles (wall and apex) is presented against absolute heart weight **(B)** and relative heart weight **(C)**. No correlation exists between relative heart weights up to 130% (*4*) and average DNA content per nucleus (R=0.08; p=0.621). All ^{14}C dated heart samples, depicted as colored dots, have relative heart weights <130% (see table S2). A positive correlation between heart weight and average DNA content per nucleus does exist only from absolute heart weights >500g and relative heart weights >130%. **(D)** Percentage distribution of ploidy levels (DNA content) of human hearts having relative weights <130% according to BMI (*4*) or **(E)** relative heart weights >130% depicted sequentially with the age of the subjects. Different grayscales indicate different ploidy levels. 2n=diploid DNA. Absolute heart weights [g] were determined as described in the Materials and Methods and in (*4*).

Figure S6. Continuous DNA synthesis in cardiomyocytes.

The age of the individual is plotted against the average age of cardiomyocyte DNA from individuals born after the bomb spike. The dotted line represents the no cell turnover scenario, where the average age of cardiomyocytes equals the age of the individual. The black line shows the best fitting for all data points (R=0.991; p<0.001). The difference

between the birth date of the person and the date corresponding to the ^{14}C level in cardiomyocyte DNA increased with the age of the individual.

Figure S7. Cardiomyocyte DNA of all ploidy levels is younger than the individual.

(A, B, C) The ^{14}C levels in cardiomyocyte DNA of all measured ploidy levels correspond to time points after the birth of the individuals. Diploid cardiomyocyte DNA is older than tetra- and octaploid DNA in all depicted subjects. **(D, E, F)** ^{14}C levels in cardiomyocyte DNA corrected for polyploidization (see supporting online text) indicate similar ^{14}C integration in diploid and polyploid cardiomyocyte DNA. The vertical bar indicates year of birth, with the correspondingly colored data point indicating the ^{14}C values for diploid (squares), tetra- and octaploid nuclei (triangles and polygons for ploidy independent values) and for all cardiomyocyte ploidy levels (dots and diamonds for ploidy independent values).

Figure S8. Y-chromosome chimerism in human heart after gender-mismatch heart or bone marrow transplantation.

Cell fusion is a potential source of non-cardiomyocyte DNA which could bias our interpretation of cell turnover. After gender-mismatched heart or bone marrow transplantation, several studies could show chimeric y-chromosome positive cardiomyocytes in the female heart. This phenomenon has been explained by cell fusion events or transdifferentiation of host/donor cells into differentiated cardiomyocytes (*5-7*). Most studies analyzing cardiomyocytes found a low level of chimerism (0% to 1.3%, median: 0.037%) with no correlation with time after transplantation (R=0.046, p=0.74)

(*5, 8-11*) nor with the age of the patient (R=0.232; p=0.086). Bayes-Genis et al. showed that the degree of chimerism in the human heart decreased by in average 38% when investigating the same individuals at 4 and 12 months after transplantation, arguing for chimerism being a temporally limited acute rather than a continuous occurring physiological phenomenon (*12*). Other studies even failed to find any evidence for cardiomyocyte chimerism (*13-15*). Two reports, however, found a much higher number of chimeric cardiomyocytes (6.4-18%) (*16, 17*) which is most likely an overestimation due to the infiltration of host-derived leukocytes into the heart and different detection techniques (*5, 11, 18*). The described low frequency of cardiomyocyte positive y-chromosomes and the transient nature of chimerism in the human heart could not explain the DNA turnover that we report here (supporting online text). Therefore neither transdifferentiation of non-cardiac stem cells into cardiomyocytes nor potential cell fusion events seems to be responsible for the observed cardiomyocyte turnover.

Table S1. Data set for all ^{14}C-dated subjects.

Table showing all data from 14 individuals whose myocardial DNA was carbon dated. DOB = date of birth, DOD = date of death, DOM = date of measurement. For a complete explanation of the terms '$\Delta^{14}C$' and 'Flow cytometry purity corrected $\Delta^{14}C$', 'C_{adj}' and 'polyploidisation independent $\Delta^{14}C$ values', refer to Material&Methods. All $\Delta^{14}C$ derived birthdates were determined by applying pMC values to the software provided on the freely accessible CALIbomb web site (http://calib.qub.ac.uk/CALIBomb/frameset.html). We used the Levin dataset and a smoothing and resolution value of one year.

Table S2. Pathological assessment and medical history of all ^{14}C-dated cases.

Comprehensive pathological assessment and medical history of all cases are presented. Heart enlargement was assessed by using tables for normal heart weights according to BMI (*4*). Hearts were considered to be enlarged if the absolute heart weight was higher than mean+ 1SD heart weight according to BMI.

Table S3. ^{14}C levels in DNA in cardiomyocyte nuclei separated based on DNA content

Table showing data from 3 subjects whose myocardial ploidy levels (DNA content) were separately carbon dated. DOB = date of birth, DOD = date of death, DOM = date of measurement. The ^{14}C values for the diploid ND54 and ND69 data points ($C_{diploid}$) were calculated based on the ^{14}C levels for higher ploidies ($C_{tetra+octaploid}$) and for all ploidy levels ($C_{allploidies}$), respectively. To validate our calculation for the ^{14}C concentration of diploid nuclei, we compared the measured and calculated diploid ^{14}C concentration of case number ND71. The calculated ^{14}C value differed <0.7% from the actual ^{14}C concentration.

$$C_{all\ ploidies} \times (ratio[\%]_{diploid} + DNAfactor \times ratio[\%]_{tetra+octaploid}) =$$

$$C_{diploid} \times ratio[\%]_{diploid} + C_{tetra-octaploid} \times DNAfactor \times ratio[\%]_{tetra+octaploid}$$

DNAfactor refers to the average DNA content per nucleus, $ratio[\%]_x$ refers to the ratio in percentage of the respective ploidy compartment (e.g. diploid). For a complete explanation of the terms 'Δ^{14}C' and 'Flow cytometry purity corrected Δ^{14}C', 'C_{adj}' and 'polyploidisation independent Δ^{14}C values', see Materials and Methods. All Δ^{14}C derived

birthdates were determined by applying pMC values to the software provided on the freely accessible CALIbomb web site (http://calib.qub.ac.uk/CALIBomb/frameset.html). We used the Levin dataset and a smoothing and resolution value of one year.

References and notes

1. A. Schmidtmann, K. Lohmann, K. Jaquet, *FEBS Lett* **513**, 289 (Feb 27, 2002).
2. D. G. Ward *et al*., *Biochemistry* **43**, 5772 (May 18, 2004).
3. Y. Zhao *et al.*, *J Mol Med* **81**, 297 (May, 2003).
4. G. L. de la Grandmaison, I. Clairand, M. Durigon, *Forensic Sci Int* **119**, 149 (Jun 15, 2001).
5. M. A. Laflamme, D. Myerson, J. E. Saffitz, C. E. Murry, *Circ Res* **90**, 634 (Apr 5, 2002).
6. S. Zhang *et al*., *Circulation* **110**, 3803 (Dec 21, 2004).
7. E. Minami, M. A. Laflamme, J. E. Saffitz, C. E. Murry, *Circulation* **112**, 2951 (Nov 8, 2005).
8. A. Deb *et al*., *Circulation* **107**, 1247 (Mar 11, 2003).
9. E. Hocht-Zeisberg *et al*., *Eur Heart J* **25**, 749 (May, 2004).
10. P. Muller *et al.*, *Circulation* **106**, 31 (Jul 2, 2002).
11. R. A. de Weger *et al*., *Bone Marrow Transplant* **41**, 563 (Mar, 2008).
12. A. Bayes-Genis *et al*., *Cardiovasc Res* **56**, 404 (Dec, 2002).
13. I. Bittmann *et al.*, *Am J Clin Pathol* **115**, 525 (Apr, 2001).
14. R. H. Hruban *et al*., *Am J Pathol* **142**, 975 (Apr, 1993).
15. R. Glaser, M. M. Lu, N. Narula, J. A. Epstein, *Circulation* **106**, 17 (Jul 2, 2002).
16. F. Quaini *et al.*, *N Engl J Med* **346**, 5 (Jan 3, 2002).
17. J. Thiele *et al*., *Pathologe* **23**, 405 (Nov, 2002).
18. D. A. Taylor, R. Hruban, E. R. Rodriguez, P. J. Goldschmidt-Clermont, *Circulation* **106**, 2 (Jul 2, 2002).

case #	Flow cytometry sorted population	sex	DOB	DOD	age	DOM	$\Delta^{14}C$	±	^{14}C derived birthdate	± years
ND60	TropI	male	Sep-33	Dec.06	73	2007	21.30	12.00	*	*
ND67	TropT	male	Aug-39	Mar.07	67	2007	20.80	9.25	*	*
ND73	TropT	male	Aug-44	Apr-07	62	2007	7.70	7.55	*	*
ND61	TropI	male	Aug-48	Jan-07	58	2007	68.60	9.42	*	*
ND51	TropT	male	Nov-55	Sep-06	50	2007	186.71	9.95	*	*
ND56	TropI	male	Feb-64	Nov-06	42	2006	430.10	10.60	1973.40	0.77
ND68	TropT	male	May-67	Mar.07	39	2007	377.83	14.81	1975.15	1.80
ND50	TropI	female	Sep-67	Sep-06	38	2006	355.70	32.20	1976.42	3.24
ND69	TropT	male	Jun-73	Mar 07	33	2007	271.14	20.79	1980.89	2.58
ND71	TropT	male	Jun-83	Mar 07	23	2007	165.60	6.17	1988.34	1.75
ND54	TropI	female	Oct-83	Oct 06	23	2006	163.60	8.40	1988.58	2.00
ND57	TropI	female	Mar-87	Nov-06	19	2006	141.20	10.20	1991.30	2.74
ND67	unsorted	male	Aug-39	Mar.07	67	2007	50.03	3.68	1956.23	0.73
ND73	unsorted	male	Aug-44	Apr-07	62	2007	32.26	4.57	1956.13	0.63
ND61	unsorted	male	Aug-48	Jan-07	58	2007	51.62	3.95	1956.23	0.73
ND59	unsorted	male	Sep-53	Dec 06	53	2006	31.70	16.00	1954.21	3.11
ND51	unsorted	male	Nov-55		50	2006	115.00	8.90	1957.63	0.34
ND56	unsorted	male	Feb-64	Nov-06	42	2006	275.70	13.40	1980.42	1.52
ND68	unsorted	male	May-67	Mar 07	39	2007	227.12	8.68	1982.70	1.44
ND69	unsorted	male	Jun-73	Mar 07	33	2007	182.92	4.85	1986.71	1.39
ND71	unsorted	male	Jun-83	Mar 07	23	2007	92.88	7.04	1998.53	2.89
ND54	unsorted	female	Oct-83	Oct.06	23	2006	144.30	6.20	1990.92	1.78
ND74	unsorted	male	Feb-87	Apr-07	20	2007	96.53	4.95	1998.01	2.40

case #	DNA content/nucleus (%) 2n=100 4n=200 8n=400	cardiomyocyte fraction in %	DNA content/nucleus weighted Flow cytometry purity in %	$\Delta^{14}C$ Flow cytometry purity corrected	birthdate Flow cytometry purity corrected	$\Delta^{14}C_{adj}$*	$^{14}C_{adj}$ derived* birthdate	polyploidisation independent $\Delta^{14}C$	polyploidisation independent birthdate	number of ^{14}C dated nuclei in millions
ND60	189.97	34.80	96.45	21.30	*	-16.44	*	19.60	*	27.70
ND67	169.20	39.45	97.00	18.84	*	-18.71	*	17.09	*	89.90
ND73	182.74	35.35	93.00	3.65	*	-22.52	*	2.79	*	45.80
ND61	212.00	48.20	98.40	69.45	*	-8.09	*	55.01	*	35.00
ND51	167.94	35.08	94.80	194.60	*	160.82	*	30.39	*	57.00
ND56	184.50	40.60	96.53	443.24	1972.67	679.88	1966.05	*	1970.73	31.00
ND68	163.21	46.35	94.04	403.08	1973.87	560.76	1968.33	*	1972.95	68.20
ND50	193.64	45.28	97.22	355.70	1976.42	520.71	1970.43	*	1973.69	33.10
ND69	175.03	29.10	96.50	279.94	1980.20	368.55	1975.43	*	1978.27	57.10
ND71	185.01	49.15	94.63	178.40	1987.14	197.07	1985.19	*	1985.45	56.50
ND54	179.02	59.57	95.50	167.38	1988.17	194.21	1985.41	*	1986.56	56.00
ND57	178.31	58.20	98.86	141.20	1991.30	162.58	1988.68	*	1989.83	37.30
ND67	169.20									>100
ND73	182.74									>100
ND61	212.00									>100
ND59										>100
ND51	167.94									>100
ND56	184.50									>100
ND68	163.21									>100
ND69	175.03									>100
ND71	185.01									>100
ND54	179.02									>100
ND74	181.20									>100

* see supplement for detailed description: 14C value correction for polyploidisation

Table S1

case #	age	cause of death	absolute heart weight at autopsy in [g]	Body Mass Index BMI	Estimated normal heart weight* according to BMI [mean+1SD]	relative heart weight [%]	Heart Enlargement*	Hypertrophy	Fibrosis
ND50	38	suicide (intoxication)	345	32	362+77	95.30	no	slight	no
ND51	50	multiple trauma	362	27	400+69	90.50	no	no	no
ND54	23	suicide (hanging)	275	18	287+74	95.82	no	no	no
ND56	42	suicide (intoxication)	387	23	370+75	104.59	no	slight	no
ND57	19	multiple trauma	220	23	287+74	76.66	no	no	no
ND59	53	suicide (intoxication)	300	19	348+58	86.21	no	no	no
ND60	73	acute myocardial infarction	485	28	400+69	121.25	yes	slight	yes
ND61	58	multiple trauma	367	22	370+75	99.19	no	slight	slight
ND67	67	acute myocardial infarction	400	25	400+69	100.00	no	yes	no
ND68	39	suicide (hanging)	362	23	370+75	97.84	no	no	no
ND69	33	suicide (intoxication)	445	34	400+69	111.25	no	no	no
ND71	23	multiple trauma	350	21	348+58	100.57	no	no	no
ND73	62	suicide (hanging)	360	17	348+58	103.45	no	no	no
ND74	20	suicide (suffocation + intoxication)	390	23	370+75	105.41	no	slight	no

*de la Grandmaison et al. 2001

Table S2

Coronar Sclerosis	Hypertension	Diabetes mellitus	Hypercholesteremia	Smoking	Cardiovascular Medication	Other Diseases	Other Medication
no	no	no	no	no	no	no	antidepressants, tranquilizers
no	no	no	not determined	no	no	no	no
no	no	no	no	no	no	no	antidepressants, tranquilizers
no	yes	no	no	no	no	psoriasis	hypnotics, tranquilizers, NSAID, opiates
no	no	no	not determined	no	no	no	antidepressants
slight	no	no	no	yes	no	COPD	benzodiazepines, opiates
moderate-severe	no	no	slight	no	nitrates	ischemic stroke 1988, old heart infarction	NSAID
slight	no	no	no	no	no	no	no
moderate	no	no	slight	no	no	no	no
no	no	no	no	yes	no	depression	hypnotics, antidepressants
no	no	no	no	yes	no	no	analgetics, anabolic steroids, benzodiazepines
no	no	no	no	yes	no	depression	antidepressants, NSAID
slight	no	no	no	no	no	ALS	benzodiazepines, opiates
no	no	no	no	no	no	no	analgetics

case #	Flow cytometry sorted population	sex	DOB	DOD	age	DOM	$\Delta^{14}C$	±	^{14}C derived birthdate	± years
ND69	TropT	male	Jun-73	Mar 07	33	2007	271.14	20.79	1980.89	2.58
ND69	TropT diploid nuclei (2n)*	male	Jun-73	Mar 07	33		301,98*		1978.82	
ND69	TropT higher ploidies (4n8n)	male	Jun-73	Mar 07	33	2007	264.10	9.70	1980.81	1.22
ND71	TropT	male	Jun-83	Mar 07	23	2007	165.60	6.17	1988.34	1.75
ND71	TropT diploid nuclei (2n)	male	Jun-83	Mar 07	23	2007	174.10	17.30	1987.26	1.97
ND71	TropT diploid nuclei (2n)*	male	Jun-83	Mar 07	23		173.03*		1987.59	
ND71	TropT higher ploidies (4n8n)	male	Jun-83	Mar 07	23	2007	164.20	4.30	1988.72	0.70
ND54	TropI	female	Oct-83	Oct 06	23	2006	163.60	8.40	1988.58	2.00
ND54	TropI diploid nuclei (2n)*	female	Oct-83	Oct 06	23		188,71*		1986.25	
ND54	TropI higher ploidies (4n8n)	female	Oct-83	Oct 06	23	2006	155.70	6.50	1990.49	0.72

case #	Flow cytometry sorted population	DNA content/nucleus weighted Flow cytometry purity in %	$\Delta^{14}C$ Flow cytometry purity corrected	birthdate Flow cytometry purity corrected	$\Delta^{14}C_{adj}$*	$^{14}C_{adj}$ derived* birthdate	polyploidisation independent birthdate	number of ^{14}C dated nuclei in millions
ND69	TropT	96.50	279.94	1980.20	368.55	1975.43	1978.27	57.10
ND69	TropT diploid nuclei (2n)*		313.22	1978.22				
ND69	TropT higher ploidies (4n8n)	93.98	271.46	1980.48	358.40	1975.85	1978.13	56.53
ND71	TropT	94.63	178.40	1987.14	197.07	1985.19	1985.45	56.50
ND71	TropT diploid nuclei (2n)	82.77	185.02	1986.27				25.50
ND71	TropT higher ploidies (4n8n)	96.60	168.14	1987.98	194.30	1985.28	1986.20	146.00
ND54	TropI	95.50	167.38	1988.17	194.21	1985.41	1986.56	56.00
ND54	TropI diploid nuclei (2n)*		195.61*	1985.60				
ND54	TropI higher ploidies (4n8n)	96.47	155.45	1989.15	186.10	1986.12	1986.86	38.50

* ^{14}C values calculated

Table S3